

March 6, 2000

Document Control Desk
U. S. Nuclear Regulatory Commission
11555 Rockville Pike
Rockville, MD 20852

Subject: Project No. 669 – Review of RETRAN-3D
Submittal of Additional Information

In a meeting with the NRC staff on December 16, 1999, the status of the NRC's review of the RETRAN-3D code was discussed. This discussion identified a number of subject areas for which additional information was required in order for the staff's review to proceed. The RETRAN Maintenance Group is submitting this letter and attachments with the intent of addressing all of the issues that are known to be outstanding. The following issues have been raised by the NRC staff during the course of the review process.

RETRAN-3D Code Versions

The RETRAN-3D MOD002 code version was originally submitted for NRC review. The MOD003 version and the associated documentation revisions were forwarded to the NRC on August 18, 1999. These revisions are designated as Revision 4 to EPRI NP-7450, Volumes 1-3, and Revision 5 to Volume 4. The NRC review should be for MOD003 only. A summary of the major differences between MOD003 and MOD002 follow:

- The 3D kinetics cross section description was changed to a piece-wise linear representation
- The channel model was added to simplify the input required to describe a core region when 3D kinetics is used
- The noncondensable gas equations of state for the 4- and 5- equation models were revised
- The 5-equation interfacial mass transfer models were revised
- Errors identified and corrected since the initial release of MOD002 were included

The documentation detailing these new models was included in the August 18, 1999 transmittal. Revisions to Volume 2 contained a description of the new cross section model and associated file structure. The corresponding cross section model description in Volume 1 was inadvertently not revised. The necessary revisions are included as Attachment 1.

DO35

RETRAN-3D Used In The RETRAN-02 Mode

RETRAN-3D can be applied in a mode that is functionally equivalent to RETRAN-02 and does not activate the major new models such as 3-D core kinetics, flowing noncondensable gas, the five-equation model, the dynamic gap conductance, accumulator, and method of characteristics models. While functionally equivalent to RETRAN-02, RETRAN-3D is more robust and faster running. This mode of application is referred to as the "RETRAN-02 mode." The following models are always active when using RETRAN-3D:

- Improved transient numerical solution (fully implicit solution of the balance equations, component models and source terms are linearized)
- Improvements to the time-step selection logic
- Fully implicit steady-state solution
- The Fanning friction model in has been revised to allow consideration of pipe roughness, rather than assuming smooth pipe
- Improved low temperature water properties

In addition, the following RETRAN-3D models can be activated by user input selection when using the code in the RETRAN-02 mode:

- The control system solution was revised to solve a coupled system of equations using a Gauss-Seidel method, rather than the single pass marching scheme. Several new control blocks improve the functionality
- The enthalpy transport model was improved by allowing multiple inlet and exit junctions and by using a mass distribution (within the half cell) that is related to the enthalpy distribution, rather than assuming a constant value
- Improved drift flux correlations
- Improved countercurrent flow junction properties
- The laminar friction model was generalized
- The combined heat transfer map has been updated with an improved set of heat transfer correlations and smoothed transitions
- The wall friction and hydrostatic head losses included in critical flow pressure (more accurate for long piping sections)
- The 1979 ANS decay heat standard with nonequilibrium precursor concentrations was added as an option

RETRAN-02-mode analyses are run using RETRAN-3D where the models and options used are limited to those that are available for use in RETRAN-02, with the exception of the model improvements described above that improve accuracy. These improve the ease of obtaining steady-state initializations, reduce the running time for transient analyses, and in some instances improve the accuracy of the solution. A RETRAN-02-mode calculation using RETRAN-3D would typically convert a RETRAN-02 input file to a RETRAN-3D input file making only the changes necessary to accommodate the minimal differences in the input structure. This conversion requires some minor formatting changes and setting model option flags to RETRAN-02 comparable models. This process has been demonstrated for 20 PWR and 7 BWR code cross comparisons included in Section VI of Volume 4. Section VII of Volume 4 includes 3 additional PWR and 1 additional BWR code cross comparisons where plant data was also available. These

cross comparisons demonstrate that RETRAN-3D can essentially reproduce the RETRAN-02 analysis results when the RETRAN-02 mode is used.

A model using any of the new RETRAN-3D features such as noncondensable gas flow, 3D kinetics, or the 5-equation nonequilibrium models, is not a RETRAN-02-mode model. Application of the new RETRAN-3D models for licensing basis analyses requires submittal for NRC review.

Scope of SER Review

The following areas constitute the scope of RETRAN-3D review that the industry requests the NRC to approve in the SER.

- 1) Use of RETRAN-3D in the "RETRAN-02 mode" for organizations with approved methodologies. This would allow RETRAN-02 users to transition to RETRAN-3D without resubmitting methodology reports.
- 2) Lift restrictions in the RETRAN-02 SER based on new RETRAN-3D capabilities or additional code validation (see Volume 4 Section III.4.4, Validation to Support Closure of RETRAN-02 TER and SER Findings).
- 3) New RETRAN-3D models
- 4) New types of licensing basis applications (beyond RETRAN-02's SER) for which submittals would be accepted for review: As examples, the following types of applications are requested to fall into this category.
 - PWR rod ejection with 3D core
 - BWR rod drop with 3D core
 - PWR steam line break with 3D core
 - PWR ATWS with 3D core
 - BWR ATWS with 3D core

Validation of New RETRAN-3D Models

Revision 5 to Volume 4 includes new and revised validation analyses using the modified models in the MOD003 code version. The results for some Volume 4 system analysis cases used to validate the 5-equation model were not modified in Revision 5. These cases include some of the heat transfer cases given in Section IV.2, the BWR-5 all MSIV closure transient given in Section VII.2.9.3 and the RETRAN-02-mode versus RETRAN-3D 5-equation comparisons shown in Section VI.4. Some justification for not revising the plotted results for these cases follows.

For the heat transfer cases, the wall heat transfer modeling has the most significant effect on the illustrated results and it was unchanged. The revised interfacial mass transfer model has only a second order affect for steady-state conditions where it reduces the liquid superheating once fully developed boiling is reached. This has a small effect on the void fraction predictions for these tests. This was demonstrated by the FRIGG cases included in Section IV.4. Here the 5-equation cases were rerun and the revised results are very similar to the MOD002 results. The FRIGG-2 results were revised in Revision 5 primarily to correct legends that were illegible and to include

several curves that were identified but not plotted in Revision 4, not because there were significant changes in the results. The FRIGG-4 results were also revised, to include an additional test and to also include results for the 5-equation model, not because of significant changes in the previous results.

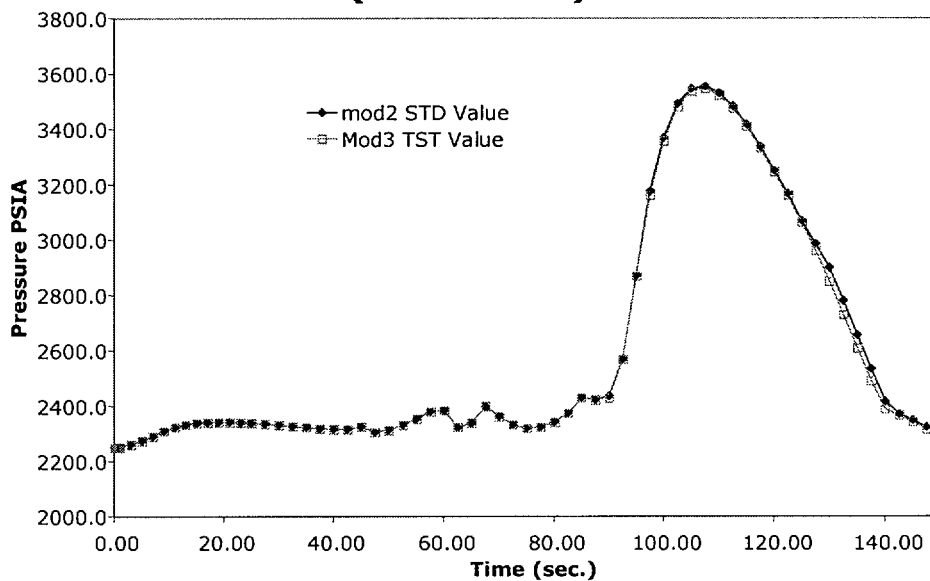
Other validation cases in Volume 4 that could be affected by the MOD003 model revisions include the BWR-5 all MSIV closure transient given in Section VII.2.9.3 and the RETRAN-02 mode versus RETRAN-3D 5-equation comparisons shown in Section VI.4. The BWR-5 case is one where the input deck is proprietary and not available. The RETRAN-02-mode versus RETRAN-3D 5-equation comparisons shown in Section VI.4 were rerun. The results are quite similar to the previous results shown in Volume 4 and were not included in Revision 5 for this reason. Attachment 2 lists the code version used to perform each validation analysis shown in Volume 4. A number of RETRAN-02-mode analyses were rerun with MOD003 but the results were not updated since there were no significant changes.

A table detailing the specific section in Volume 4 that provides validation of the new RETRAN-3D models is provided in Attachment 3. RETRAN-3D MOD002 is the code version created following the design review and the validation analysis is documented in the original submittal of Volume 4 (i.e. Revision 4). RETRAN-3D MOD003 is the code version used in the August 18, 1999 revisions (i.e. Revision 5). For each new model, the validation analyses are specified or a comment is included to indicate the status of the model. For those Volume 4 validation analyses that were run with MOD002 and do not use the new models, the baseline testing performed during the creation of MOD003 found that there were no meaningful differences between the MOD002 and MOD003 results for "RETRAN-02-mode" calculations. When the results for both codes were overlaid on a single plot, the curves were generally indistinguishable and appeared as a single curve. A few cases contained minor differences. The following plot shows a typical difference that was observed. The differences are attributed to the error corrections included in MOD003. The baseline comparisons for the RETRAN-02-mode analysis demonstrate that the results obtained with either MOD002 or MOD003 are equivalent for engineering purposes.

Validation of the 3-D kinetics model against the SPERT data was provided in the response to the second round request for additional information. The SPERT analyses were performed with an interim version of MOD002 with the new MOD003 models and some error corrections, along with a special code change to read the NESTLE cross sections directly. Validation of the 3D kinetics model against the OECD main steam line break benchmark problem is provided as Attachment 4.

The models used for the Volume 4 validation analyses are not described in a great level of detail. A judgement was made that the intent of the validation effort, which is to demonstrate that the code models can reasonably predict data, could be accomplished without providing that amount of information. The detailed information is of course available upon request for most of the analyses. It will be provided if the particular models of interest are identified. This will focus the resources on the particular models of greatest interest.

Problem 10 (Volume 34)



The validation of the Chexal-Lellouche correlation has been questioned. The database used to fit the Chexal-Lellouche correlation contained ~2000 steam-water data points, ~2000 points for the air-water, and another ~4000 points for refrigerants. Only the steam-water data is used to validate the steam-water form of the model. Additional validation of this model by the Paul Scherrer Institute was reported at the Ninth International RETRAN meeting (Attachment 5). These data comparisons used a number of steam-water heated bundle tests that were not used in the original validation of the model. These comparisons confirm the accuracy of the Chexal-Lellouche model. The validation analyses in Volume 4, as identified in Attachment 2, are a sufficient demonstration of this improvement in two-phase modeling capabilities in RETRAN-3D relative to RETRAN-02.

User Guidance for New RETRAN-3D Models

The RETRAN-3D documentation has been reviewed to identify where guidance regarding the application of the new models and options would be useful to the code user. A set of guidelines was then prepared. They do not include obvious issues, such as applying a model or correlation outside of its range of applicability as stated in the documentation, nor does it include any conditions or restrictions originating in a NRC SER. This guidance primarily includes code developer and user experience in applying new RETRAN-3D models. These user guidelines are included as Attachment 6 and will be included in the revision of the RETRAN-3D documentation that will accompany the publication of the NRC-approved version.

Licensee Submittal of RETRAN-3D Applications

It is requested that the SER approve transitioning from approved RETRAN-02 models to the same models converted for using RETRAN-3D in the "RETRAN-02 mode," for licensees with previously approved models. This transition would not require any submittals. All other RETRAN-3D applications will require submittal for NRC approval. The NRC SER will describe whatever restrictions on RETRAN-3D models and applications are to be addressed. Selection and justification of modeling and code options is the responsibility of the submitting organization.

The RETRAN Maintenance Group proposes a meeting with the NRC staff to allow further discussions on the additional information included in this letter, and to determine what actions are necessary to continue this process to a successful conclusion.

Sincerely,



G. B. Swindlehurst, Chairman
RETRAN Maintenance Group Steering Committee

Attachments (6)

Cc: Mr. L. J. Agee (EPRI)
Mr. M. P. Paulsen (CSA)
Mr. W. J. Boatwright (TXU)
Mr. J. Geosits (PPL)

Attachment 1
Volume 1 – 3-D Kinetics Cross Section Model

The net leakage vector $[L_u^{\ell mn}]$ can be represented as the difference of two adjacent face currents in the same direction as given by Eq. V.3-15.

$$[L_u^{\ell mn}] = [J_u^{\ell mn}] - [J_u^{\ell-1 mn}] \quad . \quad (V.3-15)$$

Thus, rewriting the static Eq. V.3-7 with the nodal indices suppressed for clarity and brevity, we obtain the static balance Eq. V.3-16.

$$h_y h_z [L_x] + h_x h_z [L_y] + h_x h_y [L_z] + V [\sum_T] [\hat{\phi}] = \frac{V}{k} [\chi [v \sum_f] [\hat{\phi}]] \quad . \quad (V.3-16)$$

The corresponding transient equation with time still a continuous variable yields Eq. V.3-17.

$$\begin{aligned} V [v]^{-1} \frac{\partial}{\partial t} [\hat{\phi}] = & - \{h_y h_z [L_x] + h_x h_z [L_y] + h_x h_y [L_z]\} \\ & - V [\sum_T] [\hat{\phi}] + \frac{V}{k} (1 - \beta) [\chi [v \sum_f] [\hat{\phi}]] + V \sum_{d=1}^D \lambda_d [\chi_d] \hat{C}_d \end{aligned} \quad (V.3-17)$$

where $[v]^{-1}$ is the diagonal matrix of inverse neutron speeds given by Eq. V.3-18 and \hat{C}_d is the nodal averaged precursor concentration of Eq. V.3-19, and $[\chi_d]$ is the column vector of delayed fission spectra in Eq. V.3-20.

$$[v]^{-1} \equiv \begin{bmatrix} v_1^{-1} & 0 \\ 0 & v_2^{-1} \end{bmatrix} \quad , \quad (V.3-18)$$

$$\hat{C}_d^{ijk} = \frac{1}{V_{ijk}} \int_{x_{i-1}}^{x_i} dx \int_{y_{j-1}}^{y_j} dy \int_{z_{k-1}}^{z_k} dz C_d(r,t) \quad , \quad (V.3-19)$$

and

$$[\chi] = \text{col. } \{1,0\} \quad . \quad (V.3-20)$$

The procedure used to relate the $[L_u]$'s to the $[\hat{\phi}]$'s will be discussed in Section VIII.8.6.

3.2 The Three-Dimensional Kinetics Cross-Section File

The primary source for RETRAN-3D cross sections is the CORETRAN code.[V.3-4a] Recent versions of CORETRAN have implemented a new cross-section formalism in order to address reaction types and spectrum issues of interest to fuel management groups. In general, the lattice information (from CPM-3[V.3-4b] or CASMO[V.3-4c] calculations) is processed by

CORETRAN and at given state points (i.e., point in the burn cycle) a RETRAN-3D cross-section file is written that contains instantaneous cross dependencies. That is, the cross-section dependencies for that are instantaneous. No intermediate processing codes are needed.

The RETRAN-3D cross-section file is written at the end of a CORTTRAN "burn" calculation. The RETRAN-3D model is identical in format and in functionality with the one used by CORETRAN, but the historical dependencies have been removed. That is, the RETRAN-3D model only contains the "instantaneous" dependencies, such as fuel temperature, moderator density, control fraction, or boron concentration. This reduces the size of the file as well as the cross-section calculation time for the transient analysis cases.

The cross-section functionality that forms the basis for the CORETRAN model is given by the following expression:

$$\Sigma = \Sigma (\text{EXP, TFH, DMH, CTH, BPH, ..., TF, DM, CT, B, ...}) \quad (\text{V.3-21})$$

where the independent variables can be either historic or instantaneous as defined in Table V.3-1. As a way of accounting for the contribution of each individual physical effect, the cross-section functionality is expressed by the following general sum of components:

$$\begin{aligned} \Sigma &= \Sigma_{\text{base}} (\text{EXP, DMH}) + \sum a_i \Delta \Sigma_i (\text{EXP, TFH, DMH, CTH, BPH, ..., TF, DM, CT, B, ...}) \\ &= \Sigma_{\text{base}} (\text{EXP, DMH}) + a_1 \Delta \Sigma (\text{EXP, DMH, CTH}) + a_2 \Delta \Sigma (\text{EXP, DMH, BPH}) \\ &\quad + a_j \Delta \Sigma (\text{EXP, DMH, TF}) + a_l \Delta \Sigma (\text{EXP, DMH, DM}) \\ &\quad + a_m \Delta \Sigma (\text{EXP, DMH, CT}) + a_n \Delta \Sigma (\text{EXP, DMH, B}) + \dots \end{aligned} \quad (\text{V.3-21a})$$

where a_i , $\Delta \Sigma_i$ represent the several models involved: control rod history contribution, burnable poison history contribution, and Doppler contribution. The advantage of this cross-section treatment is that it can be easily extended to include other phenomenon that users may request to model such as the interaction between the Doppler and moderator density effects.

During a burn calculation for a given depletion point, CORETRAN[V.3-4a] will prepare a table of the contributions of each effect as shown in the table below. Each cross-section set (Σ or $\Delta \Sigma$) contains information about: (a) two-group cross sections, (b) kinetics parameters, (c) assembly discontinuity factors (ADF), and (d) lattice pin power distributions.

The cross-section file for RETRAN-3D includes the core dimensions, core fuel loading information, and a three-dimensional nodal cross-section database. The fuel loading and depletion data must be obtained from a multidimensional core simulation code such as CORETRAN[V.3-4a] or SIMULATE-3,[V.3-4e] and the nodal cross-section database must be generated based on the cross-section data from lattice analysis codes such as CPM-3[V.3-4b] or CASMO-4.[V.4c] It contains two energy groups for diffusion theory constants and kinetics data.

Table V.3-1
Cross-Section Model Independent Variables

Type	Variable	Description
Historic	EXP	Exposure
	TFH	Fuel temperature history
	DMH	Moderator density history
	CTH	Control rod history
	BPH	Burnable poison history
Instantaneous	TF	Instantaneous fuel temperature
	DM	Instantaneous moderator density
	CT	Actual control state
	B	Soluble boron concentration

The cross-section file used by the multidimensional kinetics option is binary. A description of the file and its contents can be found in Section IV.2.3 of the Programmer's Manual.

Intentionally left blank.

Intentionally left blank.

3.3 Coupling Between RETRAN and the Multidimensional Kinetics Model

Previous work on nodalization studies indicate that the RETRAN-3D execution time is nearly a linear function of the total number of control volumes and junctions. When cross flow is included, the execution time approximates a cubic function of the total number of control volumes and junctions. Since a typical core region may consist of several hundred volumes and junctions, there is an upper limit to the number of channels that can be used in the core region (approximately 20-25 for a 12 axial volume core).

Because of this limitation, there are typically fewer thermal-hydraulic channels than radial neutronics assemblies and some type of modeling decisions are required. An example of a core thermal-hydraulics/neutronics overlay is given in Figure V.3-1 depicting an eight thermal-hydraulic channel model coupled to a 10 by 10 neutronics fuel assembly grid.

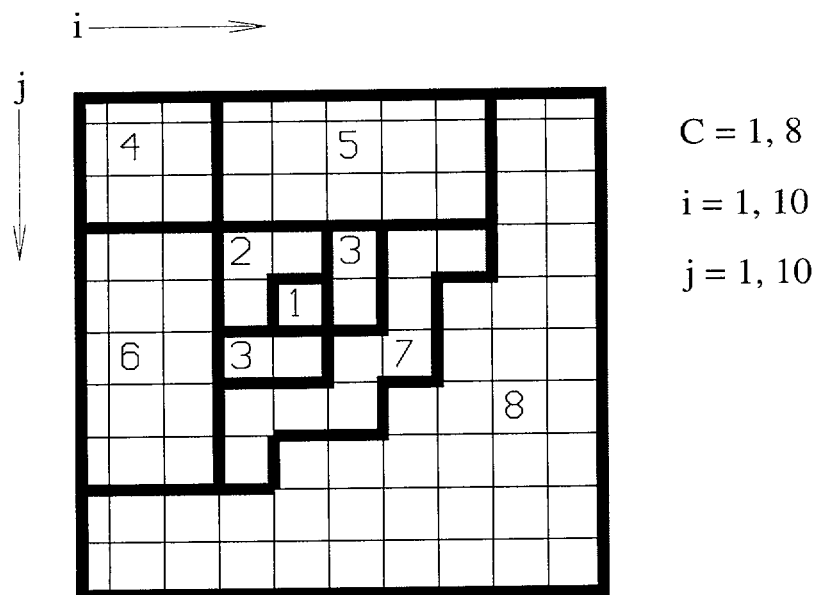


Figure V.3-1. Neutronic Thermal-Hydraulic Mapping

References

- V.2-15 Smith, K. S., "An Analytic Nodal Method for Solving the 2-Group, Multidimensional, Static and Transient Neutron Diffusion Equations", Nuclear Engineer Thesis, Department of Nuclear Engineering, Cambridge, MA, February 1979.
- V.2-16 Sutton, T. M., "Weilandt Iteration as Applied to Nodal Expansion Methods", Proceedings of the Topical Meeting on Reactor Physics and Safety, NUREG/CP-0080, p. 215, September 1986.
- V.2-17 Hansen, K. F., and Johnson, S. R., "GAKIN - A One-Dimensional Multigroup Kinetics Code", GA-7543, 1967.
- V.2-18 Cadwell, W. R., Henry, A. F., and Vigilotti, A. J., "WIGLE - A Program for the Solution of the Two-Group Space-Time Diffusion Equations in Slab Geometry", WAPD-TM-416, 1964.
- V.2-19 Di Psaquantonio, F., and Brega, E., "Three-Dimensional Analysis of Thermal Power Reactors", Proceedings of the Topical Meeting on Reactor Physics and Safety, NUREG/CP-0080, p. 574, 1986.
- V.2-20 Delp, D. L., et al., "FLARE, A Three-Dimensional Boiling Water Reactor Simulator", GEAP-4398, 1964.
- V.2-21 Meneley, D. A., Ott, K. O., and Wiener, E. S., "Space Time Kinetics - The QX1 Code", ANL-7310, 1967.
- V.3-1 Jones, D. B., "CPM-2 Computer Code Manual", ARPM-02 Documentation, Part II, Chapter 6, EPRI NP-4574, Electric Power Research Institute, 1987.
- V.3-2 Ahlin, A., and Edenius, M., "CASMO - A Fast Transport Assembly Burnup Program, User's Manual", AF-RF-76-4158, 1978.
- V.3-3 Pfeifer, C. J., and Splitz, C. J., "PDQ-8 Reference Manual", WAPD-TM-1266, 1978.
- V.3-4a Dias, A. F., et al., "CORETRAN-01 - A Three-Dimensional Program for Reactor Core Physics and Thermal-Hydraulics Analysis", Theory and Numerical Analysis, EPRI WO-3574, October 1997.
- V.3-4b Jones, D. B., et al., "CPM-3 - A Core Physics Module for the Analysis of Nuclear Fuel Assemblies Using Arbitrary Geometry Modeling", User's Manual, EPRI RP-3418, October 1997.
- V.3-4c Edenius, M., et al., "CASMO-4 - A Fuel Assembly Burnup Program", User's Manual, Studsvik/SOA-95/1, Revision 0, September 1995.

- V.3-4d Dias, A. F., et al., "CORETRAN-01 - A Three-Dimensional Program for Reactor Core Physics and Thermal-Hydraulics Analysis", User's Manual, EPRI WO-3574, October 1997.
- V.3-4e "SIMULATE-3 - Advanced Three-Dimensional Two-Group Reactor Analysis Code", User's Manual, Studsvik/SOA-95/15, Revision 0, October 1995.
- V.3-5 Dias, A. F., "Systematic Derivation, from 3-D Nodal Equations, of Simpler Models for Describing Reactor Transients", PhD Thesis, Department of Nuclear Engineering, MIT, Cambridge, MA, May 1987.
- V.4-1 Ott, K. O., and Madell, J., "Quasistatic Treatment of Spatial Phenomena in Reactor Dynamics", Nucl. Sci. Eng., 26, 563, 1966.

Intentionally left blank.

References

Intentionally left blank.

Attachment 2

CODE VERSIONS USED FOR VOLUME 4 ANALYSIS WORK

	Code Version / Organization ⁽¹⁾		
	MOD001f	MOD002	MOD003
IV SEPARATE EFFECT ANALYSES			
1.0 PRESSURE DROP			
1.1 Ferrell-McGee Pressure Drop Data		IIE	
1.2 Noncondensable Gas Pressure Drop		IIE	
2.0 HEAT TRANSFER			
2.1 Bennett, Hewitt, Kearsey, and Keays Round Tube Data		IIE	
2.2 Bennett, Collier, Pratt, and Thornton Annulus Data		IIE	
2.3 Schrock-Grossman Round Tube Data		CSA	
2.4 Condensation Analytic Solution		IIE	
2.5 Condensation in the Presence of Noncondensables		CSA	
2.6 Noncondensable Convection Heat Transfer Data		IIE	
3.0 CRITICAL FLOW			
3.1 Fauske Critical Flow Experiments		IIE	
3.2 Marviken Critical Flow Experiments		IIE	
4.0 VOID FRACTION			
4.1 FRIGG-2 Void Fraction Data			CSA
4.2 FRIGG-4 Void Fraction Data			CSA
4.3 One-Foot General Electric Level Swell Test 1004-3		IIE	
4.4 Four-Foot General Electric Level Swell Test 5801-15		IIE	
4.5 ORNL THTF Void Profile Test		IIE	
5.0 DECAY HEAT MODEL DESCRIPTION			
5.1 Results of the Analysis		CSA	
6.0 NATURAL CIRCULATION			
6.1 Purdue Thermosyphon Test		CSA	

	Code Version / Organization ⁽¹⁾		
	MOD001f	MOD002	MOD003
7.0 METHOD OF CHARACTERISTICS SOLUTION COMPARISON WITH ANALYTIC SOLUTION	CSA		
8.0 CSNI CONTAINMENT NUMERICAL BENCHMARK PROBLEM			CSA
9.0 EDWARDS PIPE EXPERIMENT			CSA
V SYSTEM EFFECTS ANALYSIS			
1.0 SHIPPINGPORT PRESSURIZER TESTS			
1.1 Loss-of-Load Tests		IIE	
1.2 MIT Pressurizer Tests		CSA	
2.0 RETRAN-3D ANALYSIS OF LOFT SMALL BREAK EXPERIMENTS LP-SB-1 AND LP-SB-2	CSA		
3.0 MULTIDIMENSIONAL KINETICS REFERENCE CALCULATIONS			
3.1 HERMITE REA Comparison			CSA
3.2 NEACRP Benchmark			CSA
3.3 PWR SLB Comparison with ARROTTA			CSA
3.4 TMI-1 Rod Ejection Accident Analyses			CSA
4.0 OMEGA ROD BUNBLE TEST			CSA

Code Version / Organization⁽¹⁾
MOD001f MOD002 MOD003

**VI COMPARISONS OF SYSTEMS ANALYSES: RETRAN-02
AND RETRAN-3D**

2.0 BOILING WATER REACTOR TRANSIENT ANALYSES

2.1 Susquehanna Feedwater Controller Failure	CSA		(2)
2.2 Susquehanna Feedwater Heater Failure	CSA		(2)
2.3 Oyster Creek Feedwater Controller Failure	CSA		(2)
2.4 Cofrentes Main Steam Isolation Valve Trip		IIE	(2)
2.5 Boiling Water Reactor ATWS	CSA		(2)
2.6 River Bend Two Recirculation Pump Trip		IIE	(2)
2.7 Peach Bottom Turbine Trip		IIE	(2)

3.0 PRESSURIZED WATER REACTOR TRANSIENT ANALYSES

3.1 ANO-2 Turbine Trip		IIE	(2)
3.2 Calvert Cliffs Steamline Break	CSA		(2)
3.3 PWR Loss of Flow	CSA		(2)
3.4 Trojan Loss of Feedwater ATWS	CSA		(2)
3.5 Prairie Island Steam Generator Tube Rupture	CSA		(2)
3.6 Three Mile Island Loss of Feedwater	CSA		(2)
3.7 Almaraz PWR Turbine Trip	UITESA		
3.8 KEPCO KNU 1 Steam Generator Tube Rupture	KEPCO		
3.9 KNU 2 Loss of Normal Feedwater	KEPCO		
3.10 Yonggwang 1 Turbine Trip	KEPCO		
3.11 TMI-1 Main Feedwater Line Break Accident		CSA	
3.12 TMI-1 Loss of Flow Accident		CSA	
3.13 TMI-1 Loss of Feedwater Accident		CSA	
3.14 TMI-1 Moderator Dilution Accident		CSA	
3.15 TMI-1 Pump Startup Accident		CSA	
3.16 TMI-1 Dropped Control Rod Accident		CSA	
3.17 TMI-1 Locked Rotor Accident		CSA	
3.18 TMI-1 Rod Withdrawal Accident		CSA	

	Code Version / Organization ⁽¹⁾		
	MOD001f	MOD002	MOD003
3.19 TMI-1 Station Blackout Accident		CSA	
3.20 TMI-1 Startup Accident		CSA	
4.0 RETRAN-02 VERSUS RETRAN-3D MODELING OPTIONS			
4.1 Boiling Water Reactor Transient Nonequilibrium Analyses			
4.1.1 Oyster Creek Feedwater Controller Failure		CSA	(2)
4.1.2 Cofrentes Main Steam Isolation Valve Trip		CSA	(2)
4.1.3 Peach Bottom Turbine Trip		CSA	(2)
4.2 Pressurized Water Reactor Transient Noneq. Analyses			
4.2.1 Trojan Loss of Feedwater ATWS		CSA	(2)
4.2.2 Prairie Island Steam Generator Tube Rupture		CSA	(2)

**VII SYSTEMS ANALYSES: COMPARISONS WITH
EXPERIMENTAL DATA**

2.0 BOILING WATER REACTOR TRANSIENT ANALYSIS

2.1 Cofrentes HPCS Injection	UITESA		
2.2 Cofrentes FW Controller Failure	UITESA		
2.3 Peach Bottom Core Stability	(3)		
2.4 Laguna Verde Generator Load Rejection	IIE		
2.5 Laguna Verde MSIV Closure	IIE		
2.6 BWR-5 Pressure Setpoint Change		TEPCO	
2.7 BWR Level Setpoint Change		TEPCO	
2.8 BWR-5 One PLR Pump Trip		TEPCO	
2.9 BWR-5 All MSIV Closure		TEPCO	
2.10 BWR-5 Generator Load Rejection with Bypass		TEPCO	
2.11 BWR-5 Single MSIV Closure		TEPCO	
2.12 Cofrentes Level Setpoint Change	UITESA		
2.13 Cofrentes Feedwater Pump Trip	UITESA		
2.14 Cofrentes Recirculation Pump Low-Speed Transfer	UITESA		
2.15 Cofrentes Turbine Trip	UITESA		

	Code Version / Organization⁽¹⁾		
	MOD001f	MOD002	MOD003
2.16 Cofrentes Gen. Load Rejection with Partial Bypass Failure	UITESA		
2.17 Vermont Yankee Stability Analysis	YAEC		
2.18 Peach Bottom Turbine Trip		CSA	
2.19 Kishiwazaki-Kariwa Unit 6 RIP Trip Test		TEPCO	
3.0 PRESSURIZED WATER REACTOR TRANSIENT ANALYSES			
3.1 KORI Nuclear Unit 1 Loss of all Off-Site Power	KEPCO		
3.2 KORI Nuclear Unit 4 Large Load Reduction	KEPCO		
3.3 Comanche Peak Steam Electric Station Load Rejection	TUE		
3.4 KORI Nuclear Unit 2 Multiple Failure Event	KAERI		

VIII DEMONSTRATION ANALYSES

2.0 COMPARISON WITH QUALITATIVE EXPECTATION

2.1 Mid-Loop Operation in PWR with Loss CSA

-
- 1 Acronym indicates organization performing the analysis (input decks not available to CSA).
 - 2 CSA rerun on MOD003 and no significant difference observed in results compared with those shown in Volume 4.
 - 3 Work preformed using MOD001

Attachment 3

Validation Analysis for New RETRAN-3D Models

The following table identifies the new models incorporated into RETRAN-3D MOD003 and the associated validation cases that are included in Volume 4. The four columns on the right indicate the sections where specific analyses are located and the numbers within the columns indicate the subsections where particular analysis results appear. Section IV contains separate effects results, Section V contains system effects results. RETRAN-02 and RETRAN-3D comparisons for RETRAN-02 mode calculations are given in Section VI. Section VII primarily contains RETRAN-3D comparisons with plant data. Several RETRAN-02 comparisons are also included.

During early discussions with the NRC staff, a request was made to withdraw the dynamic flow regime model from the review. Two other models are identified in the following table as withdrawn from review; they are the accumulator and dynamic gap conductance models.

Volume IV						
Type	Model	Volume I Data Reference	Section IV	Section V	Section VI	Section VII
Momentum Equation Wall Friction Force	Fanning Friction Factor	II-73 to II-97 III-71 to III-74	1.1, 1.2, 2.1 2.2, 2.3, 3.1	MA	MA	MA
	Laminar Friction Factor	II-73 to II-97 III-71 to III-74	6.1			
	EPRI Two-Phase Multiplier Correlation	II-73 to II-97 III-82 to III-83	(see original reference and EPRI Pressure Drop Book)			
Wall Heat Transfer Correlations	Catton and Swanson	III-106 to III-107	2.6			
	Lellouche	III-95, III-161 VIII-90 to VIII-92	2.1, 2.2, 2.3 4.1, 4.2	4.0		
Condensing Heat Transfer Correlations	Collier	III-102 to III-104		2.1		
	Chun and Seban	III-104 to III-106	2.4			

Volume IV						
Type	Model	Volume I Data Reference	Section IV	Section V	Section VI	Section VII
	Siddique	III-107 to III-110	2.5			
Critical Heat Flux Correlations	EPRI CHF Model	III-117 to III-118	(See original reference)			
State Equation Thermodynamic Properties of Water	Low Order Polynomial Expressions	II-9, II-36 to II-38 III-8 to III-18	MA	MA	MA	MA
State Equation Noncondensable Gas Properties	Ideal Gas and Dalton's Law	III-3 to III-5	1.2, 2.5, 2.6 8.0			
State Equation Transport Properties for Noncondensable Gases	Thermal Conductivity	III-6	1.2, 2.5, 2.6 8.0			
	Dynamic Viscosity	III-6 to III-7	1.2, 2.5, 2.6 8.0			
Junction Enthalpy	Countercurrent Flow	III-26 to III-29		2.1		

Volume IV						
Type	Model	Volume I Data Reference	Section IV	Section V	Section VI	Section VII
	Enthalpy Transport	III-29 to III-34 VIII-102 to VIII-110	2.1, 2.2, 2.3 2.4, 4.1, 4.2 4.5	2.1	MA	MA
	Method of Characteristics	III-65 to III-71 VIII-117	7.2			2.3, 2.17
Momentum Balance Dynamic Slip	Dynamic Slip	II-55 to II-59 II-93 to II-97 VIII-79 to VIII-87	1.1, 2.1, 2.2 2.3, 4.1, 9.1	2.1	2.4, 2.5, 2.7 3.1, 3.2, 3.3 3.5, 3.6, 3.9	3.3
Dynamic Slip Flow Regime Map	Govier Flow Regime Map	III-128 to III-129	9.1			
Momentum Balance	Colebrook Equation	III-131	1.1, 1.2 2.1, 2.2, 2.3 4.1, 4.2	2.1	2.4, 2.5, 2.6 2.7, 3.1, 3.2 3.3, 3.5, 3.6 3.9	3.3
Dynamic Slip Wall-to- Phase Friction	Dynamic Flow Regime Model	III-144 to III-145	MW	MW	MW	MW

Volume IV						
Type	Model	Volume I Data Reference	Section IV	Section V	Section VI	Section VII
Momentum Balance Dynamic Slip Interphase Friction	Taugl Model	III-140 to III-144 VIII-84 to VIII-85	AS	4.0		
	Dynamic Flow Regime	III-144 to III-145 VIII-86 to VIII-87	MW	MW	MW	MW
Algebraic Slip	Chexal-Lellouche Drift Flux	III-155 to III-160	2.1, 2.2, 2.3 3.2, 4.1, 4.3 4.4, 4.5	1.2		2.19
Five-Equation Interphase Heat and Mass Transfer	Liquid to Saturated Vapor Interface	II-59 to II-63 III-168 to III-178	(see items below)			
	Taitel-Dukler Vertical Flow Regime Map	III-169 to II-171	4.1, 4.2	4.0	4.1.1, 4.1.2 4.1.3, 4.21 4.2.2	
	Taitel-Dukler Horizontal Flow Regime Map	III-169 to II-171	9.1	4.0		

Volume IV						
Type	Model	Volume I Data Reference	Section IV	Section V	Section VI	Section VII
	Interfacial Area / Heat Transfer - Bubbly	III-171 III-175 to III-176	4.1, 4.2, 9.1	4.0	4.1.1, 4.1.2 4.1.3, 4.2.1 4.2.2	
	Interfacial Area / Heat Transfer - Slug	III-172 III-176 to III-177	4.1, 4.2, 9.1	4.0	4.1.1, 4.1.2 4.1.3, 4.2.1 4.2.2	
	Interfacial Area / Heat Transfer - Annular Mist	III-172 to III-174 III-177	4.1, 4.2	4.0	4.1.1, 4.1.2 4.1.3, 4.2.1 4.2.2	
	Interfacial Area - Transition	III-174	4.1, 4.2	4.0	4.1.1, 4.1.2 4.1.3, 4.2.1 4.2.2	
	Interfacial Area / Heat Transfer - Dispersed	III-174 III-177 to III-178		4.0	4.1.1, 4.1.2 4.1.3, 4.2.1 4.2.2	
	Interfacial Area / Heat Transfer- Stratified	III-174 -to III-175 III-178		4.0		

Volume IV

Type	Model	Volume I Data Reference	Section IV	Section V	Section VI	Section VII
Five-Equation Macroscopic Formulation		II-59 to II-63 II-98 to II-99	2.1, 2.2, 2.3 4.1, 4.2, 9.1	4.0	4.1.1, 4.1.2 4.1.3, 4.21 4.2.2	
Noncondensable Gas Mass Equation		II-63 to II-66 II-99 to II-100	1.2, 2.5, 2.6 8.0			
Heat Conduction	Dynamic Gap Conductance Model	V-8 to V-15	MW	MW	MW	MW
Power Generation Reactor Kinetics	Multidimensional Model	V-40 to V-56 VIII-176 to VIII-212		3.1, 3.2, 3.3 3.4, MSLB		SPERT
System Component Accumulator	Accumulator	VI-56 to VI-59 VIII-76 to VIII-78	MW	MW	MW	MW
Numerical Solution Methods Fluid Equations	Implicit Solution	VIII-8 to VIII-46	MA	MA	MA	MA
Pressure State Equation	Equilibrium with Noncondensables	VIII-51 to VIII-60	1.2, 2.5, 2.6 8.0			

Volume IV						
Type	Model	Volume I Data Reference	Section IV	Section V	Section VI	Section VII
	Constrained Nonequilibrium	VIII-67 to VIII-76	2.1, 2.2, 2.3 4.1, 4.2, 9.1	4.0	4.1.1, 4.1.2 4.1.3	
	Constrained Nonequilibrium with Noncondensables	VIII-67 to VIII-76	8.0			

- AS = Steady-state results are equal to corresponding algebraic slip model results
MA = Used by most or all problems
MW = Model withdrawn from review
MSLB = OECD MSLB - will be added to a future revision of Volume 4
SPERT = SPERT test results submitted to NRC - will be added to a future revision of Volume 4.

Attachment 4

OECD SLB Validation

EXERCISE 2 RESULTS, 3D KINETICS CORE MODEL WITH BOUNDARY CONDITIONS

The results presented here are a subset from the OECD/NRC Main Steam Line Break (MSLB) Benchmark. There were three phases in this benchmark:

- Phase I – Complete System Model with Point Kinetics
- Phase II – Core Model with Plenum-to-Plenum Boundary Conditions, 3D Kinetics
- Phase III – Complete System Model with 3D Kinetics

Some selected Phase II results are presented here. Phase II consisted of four hot zero power (HZZP) steady-state cases, a hot full power (HFP) case that demonstrated a return to power, and a HFP case that did not return to power. All participants' results matched well for the HZZP steady-state cases. The return-to-power HFP case results were the most interesting and are shown here for RETRAN-3D and compared to results from three other organizations using different compute codes.

In theory, the Phase II exercise provides an excellent way to benchmark 3D kinetics models since the thermal-hydraulic boundary conditions are supplied and all participants are using the same cross sections. This is in contrast to Phase I and III where differences in the system models can alter the reactor kinetics response. In Phase II, the core inlet pressure, temperature, and flow are defined, the core is single-phase liquid so differences in code two-phase models will not be observed, the core hydraulic behavior should be the same for all participants and this should only illustrate differences in 3D kinetics models. For the most part this is true, however, the results for the full power transient cases do differ slightly among participants. This document presents some selected results and discusses the reason for those differences.

The predicted axial power distributions are shown in Figures 1, 2, 3, and 4 at four times, steady state, just before scram, at the peak power after scram, and at the transient end (100 seconds). Five different predictions are shown. They are identified below:

- CSA/GPU –Computer Simulation & Analysis and General Public Utilities Analysis using RETRAN-3D
- GRS - GRS analysis using QUABOX/CUBBOX/ATHLET
- Purdue 1 – Purdue University analysis using TRAC-M/PARCS
- Purdue 2 – Purdue University analysis using RELAP5/PARCS
- Siemens – Siemens Power Company analysis using RELAP5/PANBOX2 (with internal coupling)

The fission and total transient power responses are shown in Figures 5 and 6. Results obtained by Penn State University (PSU) using TRAC –PF1/NEM are shown with the other five.

The results compare quite well for all codes, but do have some minor differences that can be explained by the following discussion.

Radial Fuel Assembly / Thermal-Hydraulic Nodal Coupling

Since the HFP cases have a radial and axial fuel and moderator temperature distribution, the coupling between the neutronic nodes and the thermal-hydraulic nodes are more significant than the HZP cases. The Benchmark Specification utilizes the TRAC code TMI model to define the thermal-hydraulic/neutronic coupling. The TRAC core model uses polar coordinates to define the radial thermal-hydraulic nodalization. Looking down on the core region, it is divided into 18 parallel “pie” shaped hydraulic channels as shown in Figure 7. Figure 8 shows the assembly mesh that is overlaid on the hydraulic mesh as given in the Benchmark Specification. Since the assemblies are square, it is not possible to overlay an assembly structure directly into pie shaped TRAC thermal-hydraulic channels without compromises. In addition, the TRAC code permits a fuel assembly to be split between two parallel flow channels and that was done in the Benchmark Specification. Since the cross sections are available on an assembly-averaged basis, the RETRAN-3D code requires flow channels to be made up of whole assemblies.

RETRAN-3D uses rectangular grids that allow the fuel assembly and hydraulic channel boundaries to match exactly; however, this does not allow the coupling methods given in Benchmark Specification to be exactly duplicated. Figure 9 illustrates the fuel assembly to hydraulic channel mapping that was used in the RETRAN-3D analysis to approximate the Benchmark Specification.

Axial Fuel Assembly / Thermal-Hydraulic Nodal Coupling

The neutronic model has 24 fueled axial nodes. The Benchmark Specifications illustrate a TRAC model with 6 axial thermal-hydraulic nodes. There is an average of 4 axial neutronic nodes in each thermal-hydraulic node. In other words, the feedback variables (moderator density and average fuel temperature) used in the cross sections, would be an averaged value over the height of these four neutronic nodes. This axial nodalization method could not be duplicated by the RETRAN-3D code, which requires an axial thermal-hydraulic node for each axial neutronic node.

It is difficult to determine how much of the differences in results are due to different fuel assembly / thermal-hydraulic coupling methods. It is believed that this is largely responsible for the differences seen in the results

Other Modeling Differences

There were small differences in the density obtained from the equation of state (EOS) from RETRAN-3D and TRAC. This is also probably true for other codes. This was observed in the HZP cases where the TRAC power distributions could be matched exactly if the TRAC density was used. These differences are probably not significant when evaluating overall system response, but do help explain why the power distributions may not match exactly.

Core Averaged Axial Power Distribution
at Time Zero
Scenario 2 - Return-to-Power

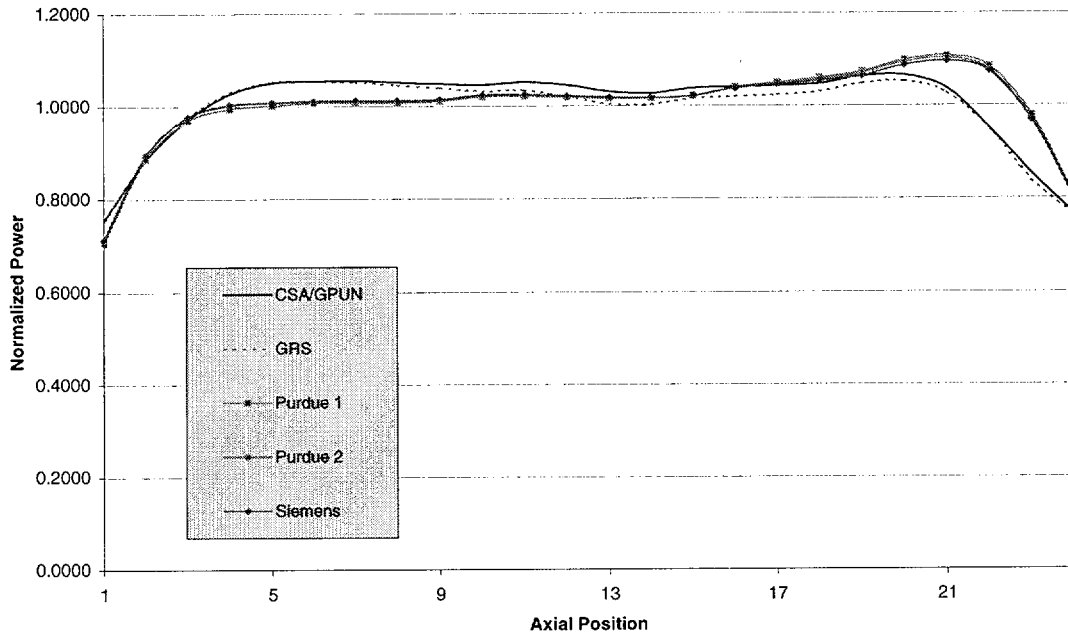


Figure 1: Time Zero Axial Power

Core Averaged Axial Power Distribution
at Time of Maximum Power Before Scram
Scenario 2 - Return-to-Power

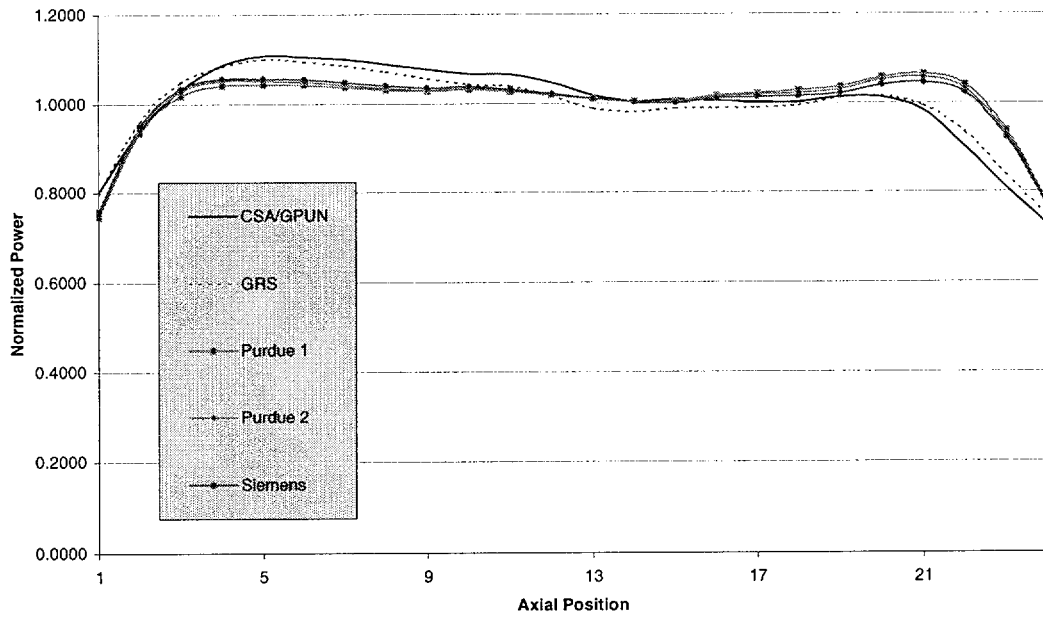


Figure 2: Pre-Scram Axial Power

Core Averaged Axial Power Distribution
at Time of Maximum Power After Scram
Scenario 2 - Return to Power

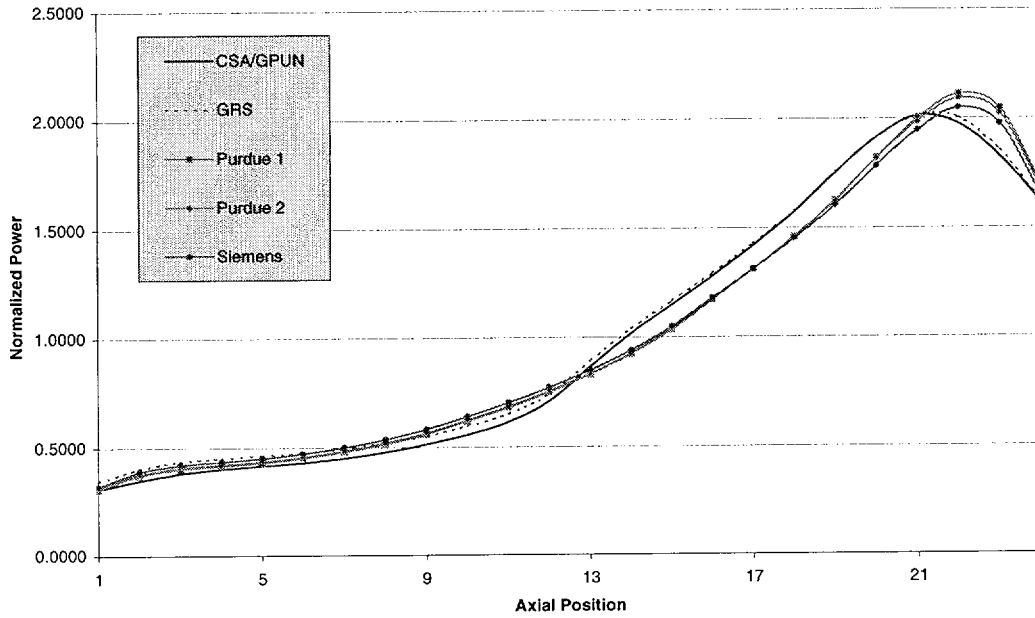


Figure 3: Post-Scram Axial Power

Core Averaged Axial Power Distribution
at End of Transient
Scenario 2 - Return to Power

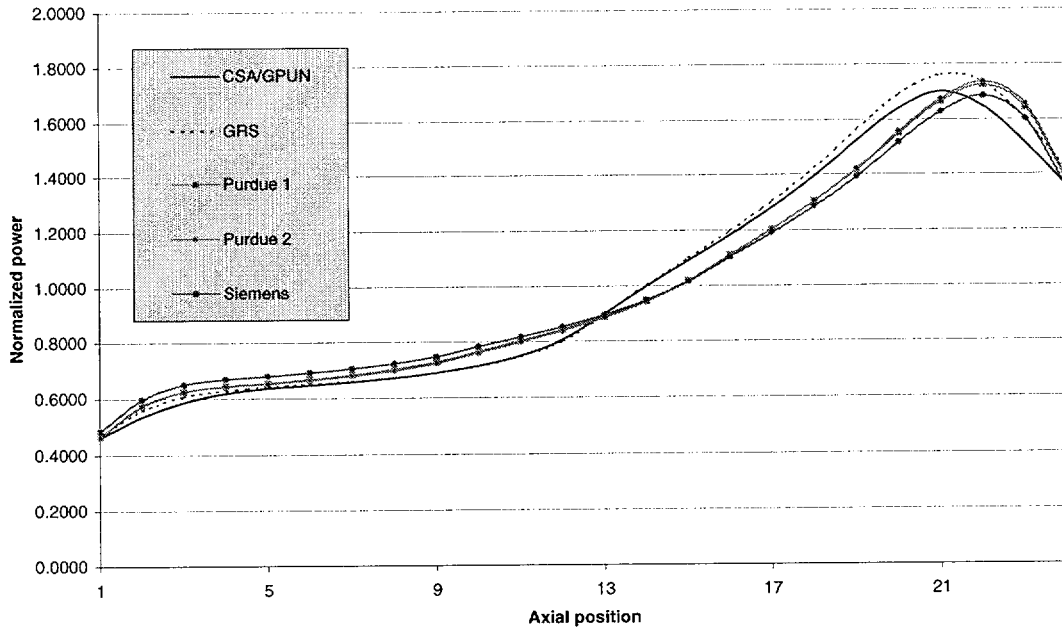


Figure 4: End of Transient Axial Power

Core Averaged Fission Power
Scenario 2, Return-to-Power

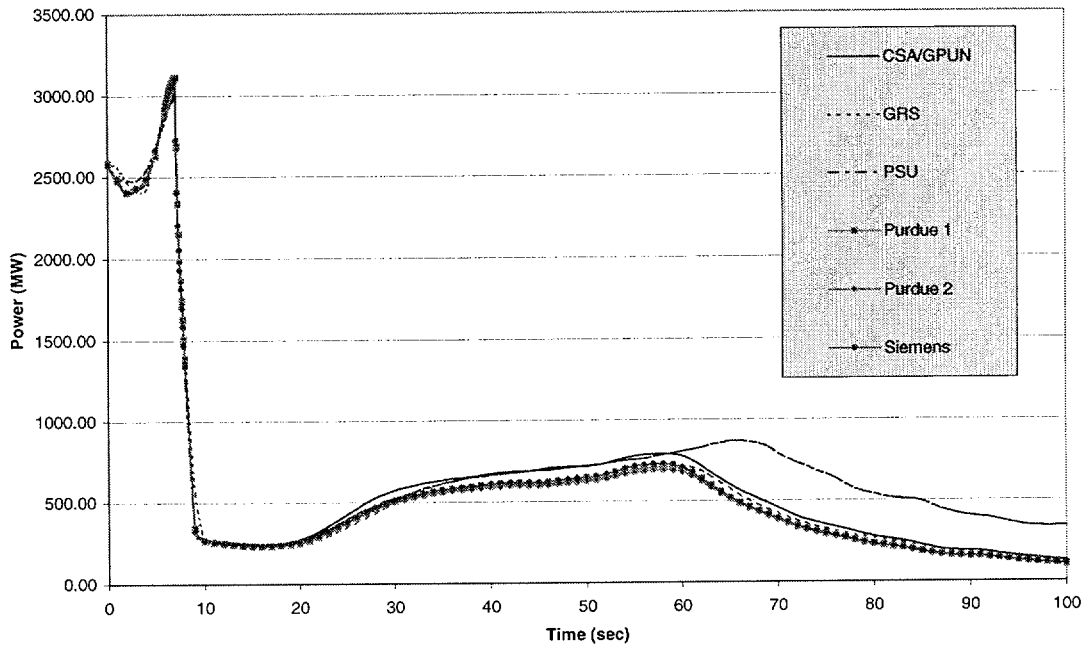


Figure 5: Fission Power

Core Averaged Total Power
Scenario 2, Return-to-Power

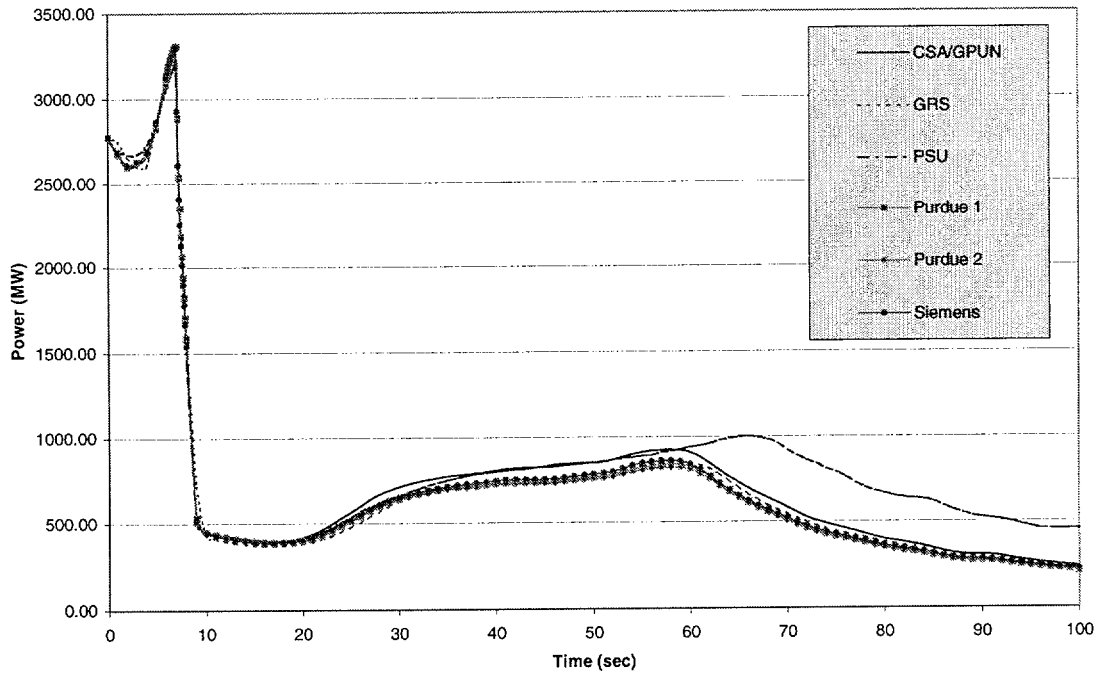


Figure 6: Total Power

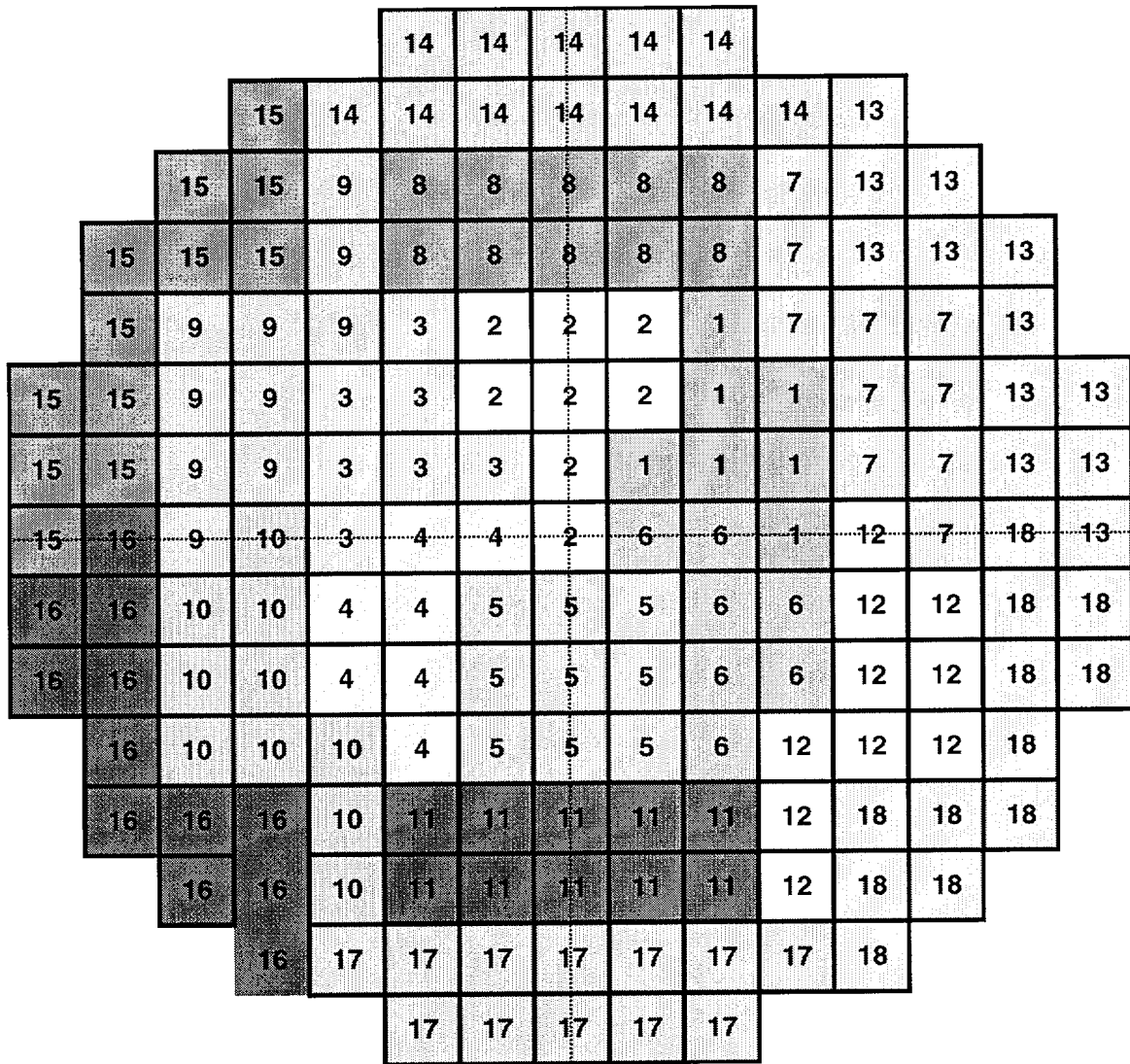


Figure 9: RETRAN-3D Core Assembly Overlay

Attachment 5
PSI paper from 9th International

EVALUATION OF THE SLIP OPTIONS IN RETRAN-3D

*D. Maier, P. Coddington,
Paul Scherrer Institute, Labor for Reactor Physics and Systems Engineering,
CH-5232 Villigen PSI, Switzerland,
Phone ++41 (0)56 310 40 62, Fax ++41 (0)56 310 23 27,
Daniel.Maier@psi.ch, Paul.Coddington@psi.ch*

ABSTRACT

Within the PSI STARS project the RETRAN-3D code is the prime tool for the system analysis of the Swiss LWRs. The range of application extends from plant transients, anticipated transients without SCRAM (ATWS) through to small break loss of coolant (LOCA) accidents for both PWRs and BWRs. RETRAN-3D offers the user several solution schemes for the two-phase flow field, and this can play a major role in the analysis of the applications described above. For the user to confidently choose the "best" option for a particular calculation, a systematic evaluation of the predictive quality of the different solution methods must be performed.

This paper describes a systematic evaluation of the slip options available in RETRAN-3D using the 3-/4-equation models as well as an initial assessment of the 5-equation model against a wide range of rod bundle void fraction data. This is important since, for example the correct prediction of the interfacial friction and consequently of the void fraction within a reactor core is necessary for the prediction of such phenomena as core uncover and dryout under both transient and accident conditions, and the core power level and distribution during an ATWS. The data base used for this analysis includes information on 83 rod bundle experiments from 9 experimental facilities performed in 4 different countries. The range of parameters extends from those appropriate to normal operation in BWRs to small break LOCA conditions in both PWRs and BWRs. The majority of the experiments were performed under steady state inlet flow conditions at a given system pressure with varying amounts of subcooling. However some data is also included from low pressure boil-up and boil-down transients. For the boil-up experiments the controlling parameter is a constant collapsed liquid level, while in the boil-down experiments the test section liquid is allowed to slowly boil away.

In the 3-equation model two drift flux correlations are available (Zolotar-Lellouche and Chexal-Lellouche) for determining the liquid/vapor slip, in addition to homogeneous flow (no slip). The 4-equation model includes an additional momentum equation (referred to as the dynamic slip equation). The form of the interphase friction used in this equation comes from either an "inversion" of the above two void correlations or from a "flow regime dependent slip option". The 5-equation model includes a vapor mass conservation equation which controls the vapor mass additionally to the total mass conservation and therefore does not necessarily require both phases to be in thermal equilibrium.

The results of the assessment using the 3-/4-equation model show that all of the options provide an excellent prediction of the experimental data for high pressures and high mass fluxes (i.e. typical of BWR normal operation). However there is a progressive worsening of the predictive quality of all options, except that of the Chexal-Lellouche correlation, as first the inlet flow rate is reduced at high pressure, and secondly the system pressure is reduced. At low mass fluxes, i.e. typically less than 50 kg/m²s, and pressures below about 2 MPa there is some consistent overprediction of the void fractions by the Chexal-Lellouche correlation, while at very low pressures and very low mass fluxes, i.e. less than 0.3 MPa and 10 kg/m²s, the code fails to reach a converged solution. Since the majority of the experiments analyzed were steady-state experiments there is no substantial difference between the 3-equation and 4-equation model predictions. When compared against the total data base the 4-equation model using the Chexal-Lellouche correlation results in a mean error of -0.008 and a standard deviation of 0.07.

An initial assessment of the 5-equation model against experimental data with significant inlet subcooling shows that the subcooled boiling model underpredicts the void fraction for qualities less than about 3 percent. At higher qualities, i.e. when the liquid phase has reached saturation temperature, the predictions are consistent with those of the 3-/4-equation model.

INTRODUCTION

Application of computer codes for transient system analyses of LWRs is an important aspect in modern nuclear safety analysis. Validation work gives the necessary confidence in the adequacy of these codes for modeling true physical processes. Thermal-hydraulic transient analysis codes such as RETRAN-3D [i] offer the user many "input model options" which determine the calculation methods used for the subsequent analysis. For the user to confidently choose the most appropriate options for a particular application, the limitations and benefits of these options must be known. Therefore a systematic evaluation of the predictive quality of the code for the options of interest must be performed.

The main tool for the system analysis of PWR (Pressurized Water Reactor) and BWR (Boiling Water Reactor) thermal-hydraulic and reactor physics transients for the STARS¹ project is RETRAN-3D. Independent code assessment has been performed in order to enhance the code validation. This was done in the form of an extensive investigation of the options available in RETRAN-3D for calculating the liquid/vapor slip and subsequently the void fraction distribution within rod bundles. This area of study was selected, since void fraction distribution in a reactor core is a crucial factor for the correct prediction of phenomena such as core uncover and dry-out during accidents, and power level and distribution during an anticipated transient without SCRAM (ATWS), all of which play an important role in the overall simulation of nuclear reactor transients.

A systematic evaluation of the options within RETRAN-3D for calculating the liquid/vapor slip, against a wide range of rod bundle void fraction data was performed. The data base includes information on 83 experiments from 9 experimental facilities located in 4 countries. The range of experimental parameters extends from those appropriate to normal operation in BWRs to small break loss of coolant accident (LOCA) conditions in both PWRs and BWRs. The majority of the experiments were performed under steady-state inlet flow conditions at a given system pressure and power, with varying amounts of subcooling. However some data is also included from boil-up and boil-down transients primarily at low pressure. For the boil-up experiments the controlling parameter is a constant collapsed liquid level, while in the boil-down experiments the test section liquid inventory is allowed to slowly boil away.

In this paper we present the results of the analysis of these rod bundle experiments using the various slip models available in RETRAN-3D. The strengths and weaknesses of the different options are assessed, and experimental conditions under which the code displays difficulties or produces inaccurate results are indicated.

EXPERIMENTAL DATA

The collected experimental data is recent rod bundle void fraction data taken from test facilities in France (PERICLES), Japan (BWR4x4, BWR8x8, LSTF², PWR5x5, TPTF³), Switzerland (NEPTUN) and the UK (ACHILLES, THETIS). Most of the data was previously used for a review of a wide range of void correlations by Maier and Coddington [ii]. A detailed list of the experimental facilities and selected parameters is given in table 1, and a short description of each facility and the experiments analyzed is given below.

ACHILLES [iii]

The ACHILLES Rig at Winfrith Technology Centre, UK, consists of a model PWR fuel assembly with 69 heated rods. The facility was used for single-phase flow, low flooding rate reflood and low pressure level swell experiments. The data used for this study is from the level swell experiments.

BWR4x4 [iv]

This Japanese facility with 4x4 rods has a radial power distribution which is highly biased to four rods in one corner. The main purpose of the test facility was to evaluate void fraction measurements made using both an advanced X-ray computed tomography (CT) scanner, similar to those used in medical research, and an X-ray densitometer.

¹ STARS: Simulation models for the Transient Analysis of the Reactors in Switzerland

² LSTF: Large Scale Test Facility

³ TPTF: Two-Phase Flow Test Facility

Table 1. Overview of the experimental facilities and the significant parameters.

Facility Name	ACHILLES	BWR4x4	BWR8x8	LSTF	NEPTUN	PERICLES	PWR5x5	THETIS	TPTF
reference	[iii]	[iv]	[v]	[vi]	[vii]	[viii]	[ix]	[x]	[xi]
year of publication	1989	1990	1991	1990	1988	1985	1996	1984	1994
facility type	PWR	BWR	BWR	PWR	LWHCR ⁵	PWR	PWR	PWR	PWR
country	UK	Japan	Japan	Japan	Switzerland	France	Japan	UK	Japan
experiments	2	4	10	11	3	8	7	20	18
data points	26	20	52	29	11	47	87	145	77
heated length [m]	3.7	3.7	3.7	3.7	1.7	3.7	3.7	3.6	3.7
rods (heated)	69 (69)	16 (16)	64 (62)	1104 (1008)	37 (37)	357 (357)	25 (25/24)	49 (49)	32 (24)
rod diameter [mm]	9.5	12.3	12.3	9.5	10.7	9.5	9.5	12.2	9.5
hydraulic diameter [mm]	13	12	13	13	4	11	16	13	10
axial power distribution	chopped cosine	uniform	uniform / chopped cosine	chopped cosine	chopped cosine	chopped cosine	uniform / chopped cosine	chopped cosine	uniform
inlet flow subcooling [K]	18 / 24	0*	9-12	0*	0.5-3	20 / 60	20-90	25-157*	5-35
pressure [MPa]	0.1 / 0.2	0.5 / 1.0	1.0-8.6	1.0-15.0	0.4	0.3 / 0.6	7.4-16.6	0.2-4.0	3.0-11.8
mass flux [kg/m ² s]	7.8/8.3*	833 / 1390	284-1988	2.2-84*	42 / 91	9-30*	2222-3056	3-18*	11-189
avg. heat flux [kW/m ²]	11	350-743*	225-3377*	5-45	5/10	11-40	733-1282	4-11	9-170

⁵ Light Water High Conversion Reactor

* estimated values (see text)

BWR8x8 [v]

Experiments at this larger facility (8x8 fuel rods) were designed for void fraction measurements under BWR operating conditions. These experiments were performed by the same group using the same measuring techniques as for the BWR4x4 experiments. Data is available from experiments with both a uniform axial power distribution and a chopped cosine distribution.

LSTF [vi]

The LSTF² in Japan is a scaled model of a Westinghouse-type PWR containing a full-length 1104-rod electrically heated bundle, with the rods arranged in 69 4x4 arrays. It is designed for pressures up to 18 MPa. The experiments including void fraction measurements were performed under the ROSA-IV⁴ program at JAERI⁵, for the purpose of studying SBLOCAs and transients.

NEPTUN [vii]

The NEPTUN facility at Würenlingen, Switzerland, is a test facility with 37 heated rods, designed for reflooding and boiloff experiments. The series of experiments used in this analysis were LWHCR⁶ low flow experiments. The special feature of LWHCR tests is the small pitch between the heated rods, resulting in a very small equivalent hydraulic diameter (see Table 1).

PERICLES [viii]

Experiments performed at the PERICLES facility in France were performed to study 2-D effects in PWRs. The core section consists of three 7x17 arrays of heated rods. Level swell experiments with both radially uniform and non-uniform power distributions were used for the present study.

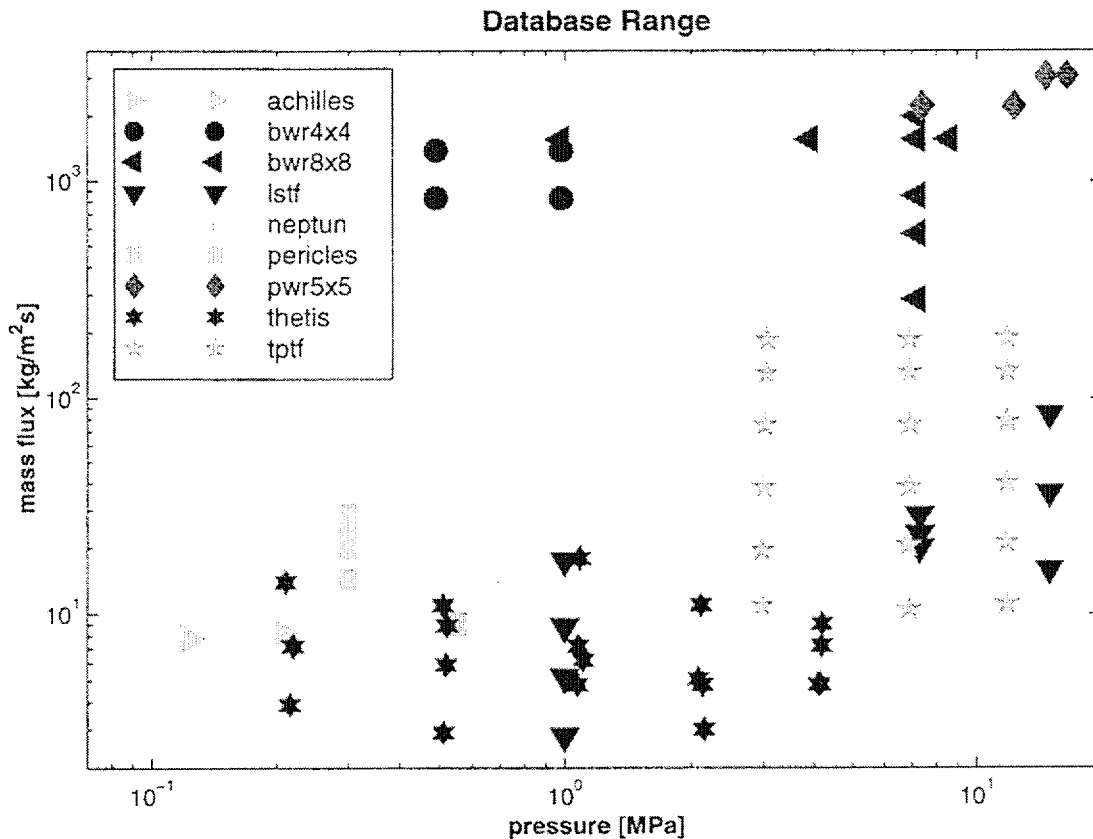


Figure 1. Pressure and mass flux range of the analyzed experiments.

⁴ ROSA-IV: Rig of Safety Assessment Number 4

PWR5x5 [ix]

These experiments were performed at high pressures (7-17 MPa) with high mass fluxes (200-3000 kg/m²s) and significant subcooling (20-90 K). The test section consisted of 25 heated rods arranged in a square 5x5 assembly with dimensions similar to those of a 17x17 PWR assembly.

THETIS [x]

The THETIS rig at Winfrith in the UK consisted of a model PWR fuel assembly with 49 heated rods, containing a severe partial blockage. The experimental data used for the analysis is from the boil-down and boil-up level swell experiments.

TPTF [xi]

The TPTF³ in Japan is also part of the ROSA-IV⁴ program at JAERI⁵. The central 24 of the 32 rods in the circular core section are heated. The experimental data is from boil-off experiments covering a wide range of pressures and mass fluxes.

Figure 1 displays the boundary conditions of the analyzed experiments as a function of the two important parameters, pressure and mass flux. As can be seen the data base includes experiments covering a wide range of pressures and mass fluxes. In addition it contains experiments from different facilities with similar experimental conditions, allowing the confirmation of observed characteristics against data from different sources.

The data can be divided into three distinct groups determined by the type of experiment performed. In the following sections these three types are labeled steady-state, boil-up and boil-down experiments respectively. The experimental procedures are briefly described below.

STEADY-STATE EXPERIMENTS

The majority of the experiments analyzed were performed under steady-state conditions with the power, inlet mass flow and subcooling at constant values. The parameters of these experiments span the whole range of the data base, with the exception of very low mass fluxes (< 10 kg/m²s) and very low pressures (< 0.3 MPa). The power input into the fluid is low for low mass flows to prevent the top of the heated rods from drying out, and high for high mass flows to ensure that sufficient voiding occurs.

The BWR4x4 and BWR8x8 facilities simulate, as the name suggests, BWR heater rod assemblies and were specifically designed for studying void fraction measurement techniques and void distribution. The PWR5x5 and TPTF³ facilities have rod assemblies typical of PWRs, and were both used for separate effects tests. The NEPTUN facility is a somewhat special case as it was originally used for PWR reflood experiments and then redesigned with a tightly packed rod assembly for use in LWHCR⁶ research. This arrangement produces a very small equivalent hydraulic diameter of 4 mm. The analyzed NEPTUN experiments were from the latter data set.

BOIL-UP EXPERIMENTS

The second group of experiments consists of boil-up experiments, where the controlling parameter is a constant collapsed liquid level. The parameters of these experiments are limited to low flows (< 100 kg/m²s) but extend over almost the complete pressure range of the experiments analyzed (0.2 - 15 MPa). The power into the fluid is kept constant at all times while the inlet flow varies as required to maintain the desired collapsed liquid level.

For the PERICLES experiments and the THETIS boil-up experiments, which are both facilities with PWR-type fuel assemblies, the downcomer level was maintained at a constant elevation, allowing flow from the downcomer into the test section to replace the liquid being boiled away. For the boil-up experiments at the LSTF facility, which was designed for PWR integral tests, the test section was always completely covered by the water-vapor mixture.

⁵ JAERI: Japan Atomic Energy Research Institute

⁶ LWHCR: Light Water High Conversion Reactor

BOIL-DOWN EXPERIMENTS

The common feature of the boil-down experiments is that the liquid inventory in the test facility is gradually boiled away. The mass flows in these experiments are very low ($< 10 \text{ kg/m}^2\text{s}$), since the only flow coming into the test section consists of liquid flowing from the downcomer into the test section as the total inventory decreases. The pressures of these experiments vary from 0.1 to 4 MPa.

In the THETIS boil-down experiments the initial mass flow into the test section was stopped while maintaining a constant power level. The procedure for the ACHILLES experiments was somewhat different, since the test section was initially filled with slightly subcooled water and the power was then increased up to the desired value. Both the THETIS and the ACHILLES facilities were reflood facilities with the heated rods arranged in an array similar to that of a PWR assembly.

RETRAN-3D CODE OPTIONS

Two different approaches are used by the RETRAN-3D code for calculating the two-phase flow field, the 3-equation and the 4-equation model. The 3-equation model solves the 3 conservation equations of total mass, momentum and energy and uses a drift-flux correlation to directly determine the slip velocity. The 4-equation model solves an additional momentum equation (in fact a velocity difference equation) which is referred to as the dynamic slip equation.

The 5-equation model in RETRAN-3D includes an additional equation for vapor mass conservation, allowing the fluid contents in a control volume to be in thermal non-equilibrium. This option was not studied in detail since it relies on the interfacial mass and energy transfer model which is currently being improved [xii].

3-EQUATION MODEL

Besides the homogeneous flow model (no slip) RETRAN-3D includes two drift-flux models for the calculation of the liquid/vapor slip. These are the Zolotar-Lellouche [xiii] and the more recent Chexal-Lellouche model [xiv]. The Chexal-Lellouche model was developed using a wide range of experimental data including rod bundle data at pressures and mass fluxes similar to those of the experiments analyzed here. As described above these drift-flux models are used to determine the slip velocity separately from the solution of the conservation equations.

4-EQUATION MODEL

The dynamic slip equation used for the 4-equation solution is obtained by subtracting the gas phase from the liquid phase momentum equation. For vertical flow the interphase friction term in the dynamic slip equation is evaluated from either the "taugl" model (see below) using one of the two drift-flux models mentioned above or from "flow regime dependent" constitutive models. The flow regime dependent option uses the flow regime map by Bennett et al. [xv] for vertical flow, to determine which constitutive model should be used to calculate the interphase friction as a function of the local conditions. If one of the drift-flux model options is selected the technique used to determine the interphase friction is the "taugl" model based on the approach of Andersen and Chu [xvi]. In the "taugl" model the interphase friction term, the form of which was developed by Ishii [xvii], is determined based upon a solution of the drift-flux model by Zuber and Findlay [xviii] neglecting the wall friction terms. The exact procedure is described in the RETRAN-3D manual in section 5.1.3 ([i], pages III-140 - III-144). This model has the advantage, over the flow regime dependent slip option, of removing the limitations associated with the discontinuous form of the interphase friction term as the flow regime changes.

5-EQUATION MODEL

In addition to the equilibrium equations used for the 3- and 4-equation models, a vapor mass conservation equation is solved when the 5-equation model is selected. The option used for the evaluation of the liquid/vapor slip in the 5-equation model can be any of the 3- or 4-equation model slip options. For the solution of the mass and energy conservation equations the vapor in any two-phase node is assumed to be at saturation. Thus the difference when using the 5-equation model for predicting void profiles arises from the fact that either vapor can be produced before the liquid reaches saturation temperature (subcooled boiling), or that cold water injected into a single-phase vapor node is not immediately heated up to saturation. Since the model for interfacial mass and energy transfer in RETRAN-3D which strongly influence the phenomena described above, is currently being

improved [xii], the current assessment of the slip options using the 5-equation model is not definitive. Therefore the analysis presented here should only be viewed as a preliminary result.

INPUT MODELING

The test section of the experimental facilities was modeled using a single channel with a “fill junction” at the bottom and a “time dependent volume” at the top (figure 2). Core conductors were used to simulate the heated rods and the power input. The fill junction was used to set the inlet mass flux and subcooling, while the system pressure was set using the time dependent volume. The nodalization was selected such that the node locations corresponded to the power distribution steps for experiments with cosine shaped power profiles and with the locations of the differential pressure measurements for the experiments with uniformly distributed power.

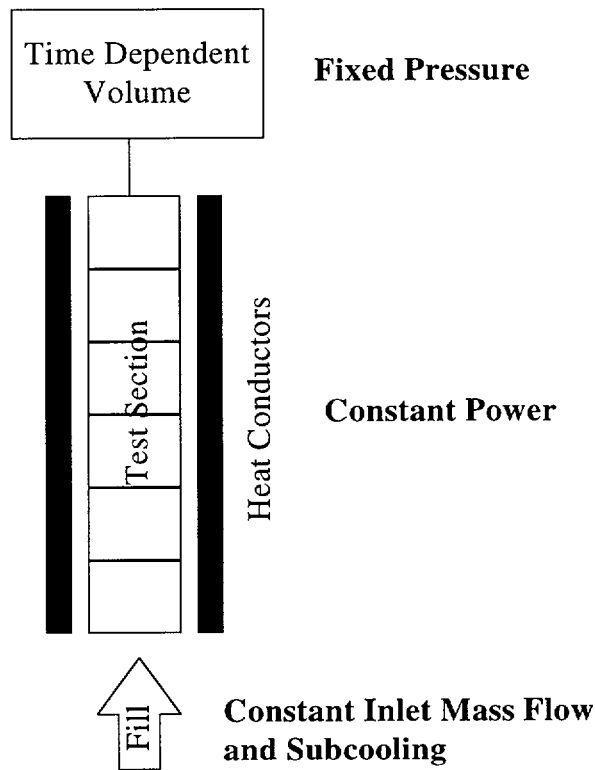


Figure 2. Nodalization diagram.

RETRAN-3D offers the user two modes of operation, steady-state and transient. The one used for the majority of the experiments was the steady-state initialization. Only the boil-down experiments were modeled as transients. The modeling procedures used for the three different groups of experiments are described below.

STEADY-STATE EXPERIMENTS

For the NEPTUN, PWR5x5 and TPTF experiments the pressure, the inlet mass flux and subcooling, and the total power were available, and input directly into the corresponding components of the RETRAN-3D model. For the BWR4x4 and BWR8x8 experiments the power input was not known and was selected such that the exit quality was slightly higher than in the experiment. For the RETRAN-3D analysis this assumption is acceptable, since the measured data of these experiments is presented as void fraction vs. quality and not vs. elevation, as is the case for the other steady-state experiments. The calculations of the steady-state experiments with RETRAN-3D were simple and straightforward, and were accomplished using the RETRAN-3D steady-state initialization procedure without any problems.

BOIL-UP EXPERIMENTS

The facilities where boil-up experiments were performed, were designed as reflood facilities (THETIS / PERICLES) and as an integral facility (LSTF), and were not equipped to measure low inlet flows into the heated test section. Therefore the following procedures were developed to make the optimum use of the information available, which included total power, pressure and collapsed liquid level.

The inlet flow into the test sections at the THETIS and the PERICLES facilities was modeled such that the collapsed liquid level calculated by the code corresponded to the given experimental value. This required a number of iterations to find the "correct" inlet mass flux. The mass fluxes determined in this manner do not necessarily represent the experimental values, since the collapsed liquid level is calculated by the code, including any deficiencies of the code models. Therefore the calculated void fractions may well match the experimental data, despite having used a "wrong" inlet mass flux for the input model.

A different approach was used for the LSTF facility since the collapsed liquid level was not known for these experiments. In order to obtain the correct inlet mass flux, the correlation presented by Anoda et al. [vi] was coded and the inlet flow rate was adjusted until the void fractions calculated using this "Anoda" correlation corresponded to the predicted void fraction values presented in the paper by Anoda. Additionally, the same procedure was performed for the Cunningham and Yeh [xix] correlation for which Anoda also presents void fraction predictions. The close agreement of the inlet mass fluxes determined from the independent comparison of the void fraction predictions using these two correlations, show that the values for inlet mass flux and subcooling determined in this way are close to the experimental values.

BOIL-DOWN EXPERIMENTS

The THETIS boil-down and the ACHILLES experiments were the only transient experiments analyzed. In both cases the liquid inventory was slowly boiled away at a constant pressure and constant power. In the THETIS experiments the initial inlet flow which kept the liquid level constant was suddenly stopped. Following this, the downcomer inventory gradually flowed into the test section partially replacing the liquid boiled away. The ACHILLES test section was initially partially filled with subcooled liquid, and power was then applied to the heater rods. Again the liquid inventory slowly flowed from the downcomer to the test section as it boiled away. The initial collapsed liquid level for the THETIS experiments was known and the corresponding inlet flow was determined in a manner similar to that described above for the boil-up experiments. For the ACHILLES experiments the starting point of the boil-down transient was not known, i.e. the amount of liquid in the test section, before the power was applied, was not provided.

Due to problems predicting data at low pressures (< 0.3 MPa) in combination with low mass fluxes (< 10 kg/m²s), conditions under which most of the boil-down experiments were performed, no successful void predictions could be produced for the ACHILLES data and for the lowest pressure THETIS experiments. These problems are described in more detail below.

SLIP MODEL PREDICTIONS

3-EQUATION OPTIONS

Figures 3 and 4 show the results of the analysis using the two drift-flux models available within the RETRAN-3D 3-equation solution, the Zolotar-Lellouche and the Chexal-Lellouche correlation. For completeness the plots also include results for the homogeneous flow option (no slip). The plot titles display the name of the experimental facility as well as the pressure and mass flux of the experiment analyzed. The examples shown here are selected to represent the trends and observations found for most of the data analyzed.

As can be seen in figure 3 both drift-flux options give equally good results for an experiment at BWR normal operating conditions 7.2 MPa - 1600 kg/m²s, as for example in this BWR8x8 experiment. However at lower mass fluxes (18 kg/m²s) and lower pressures (1.0 MPa), as shown for example in figure 4 (LSTF), an overprediction of the data is observed for all model options. While the Zolotar-Lellouche prediction is very poor, the Chexal-Lellouche correlation produces a closer agreement. Comparing the predictions to the experimental data from different facilities with varying pressures and mass fluxes the void fractions appear to be increasingly overpredicted as both pressure and mass flux are decreased (see below).

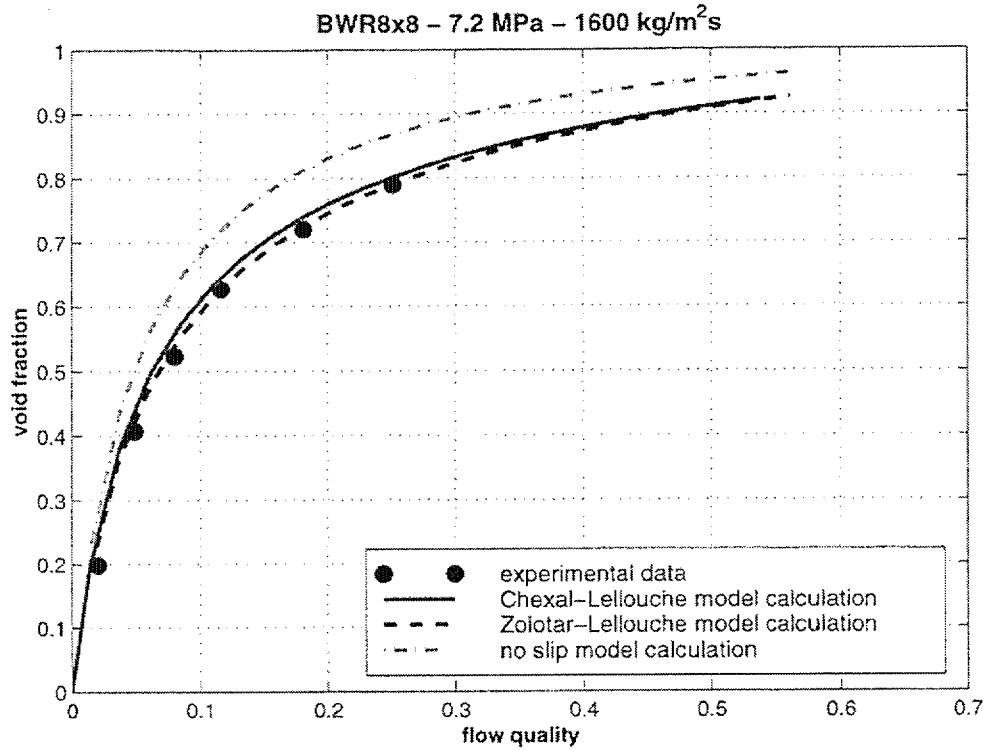


Figure 3. Prediction of a BWR8x8 experiment using the 3-equation model options.

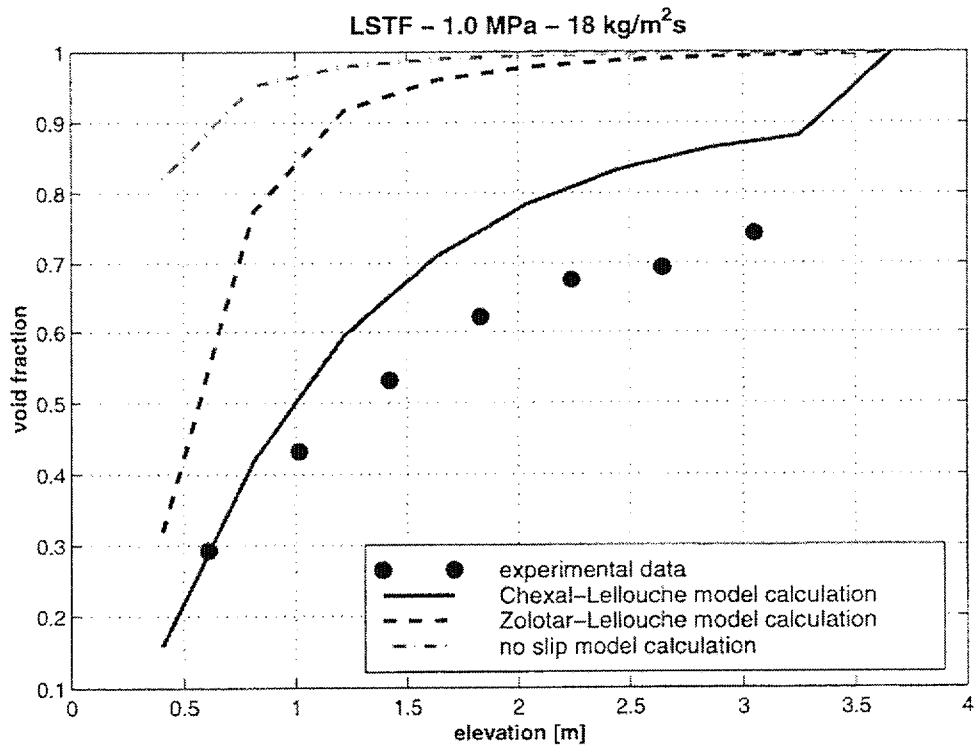


Figure 4. Prediction of a LSTF experiment using the 3-equation model options.

4-EQUATION OPTIONS

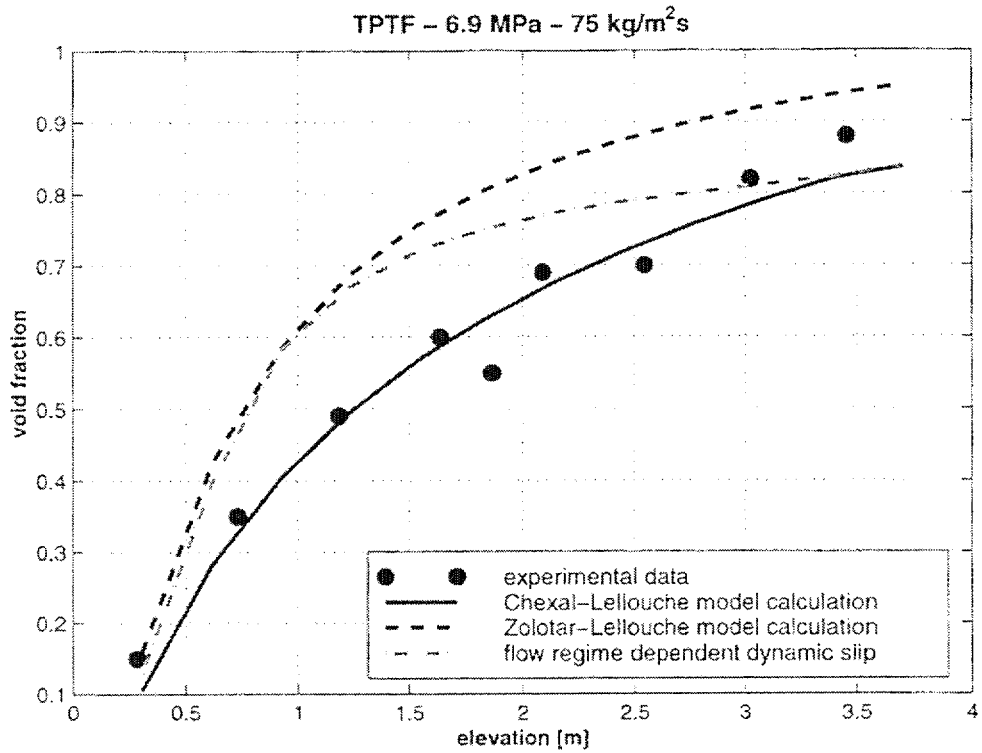


Figure 5. Prediction of a TPTF experiment using the 4-equation model options.

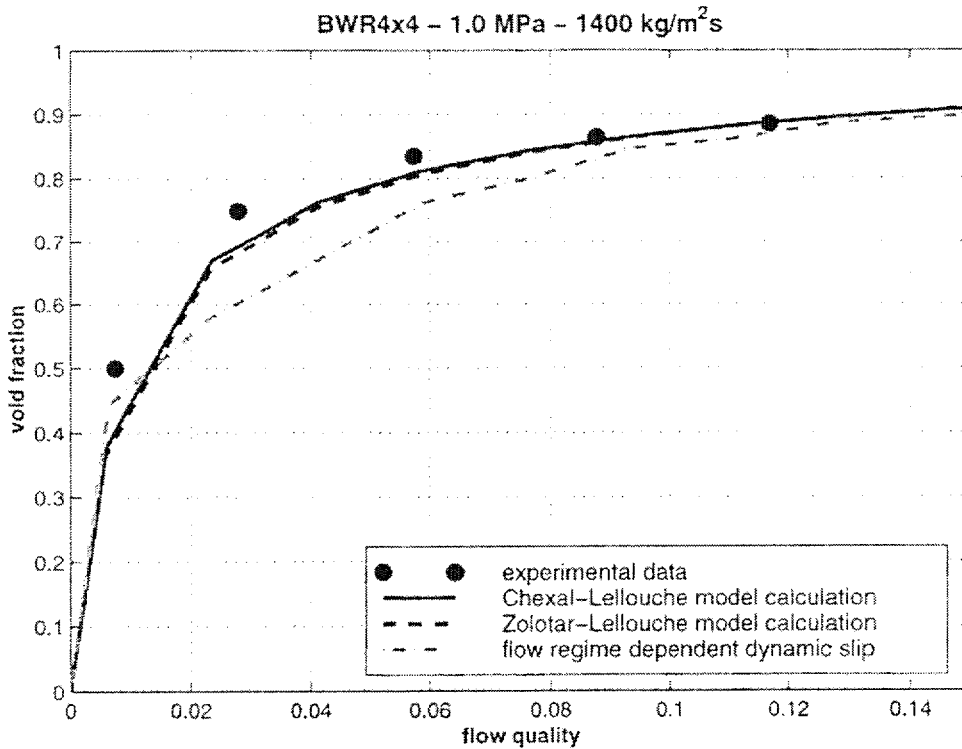


Figure 6. Prediction of a BWR4x4 experiment using the 4-equation model options.

The two drift-flux models available as options for the 3-equation solution (Zolotar-Lellouche and Chexal-Lellouche) can also be selected in the context of the 4-equation model, where the interphase friction term in the dynamic slip equation is determined using the “taugl” model. Additionally there is a “flow regime dependent” slip option, which evaluates the interphase friction term according to the flow regime present in a given control volume. In figures 5 and 6 RETRAN-3D predictions using the 4-equation model options are compared to the experimental data.

The superiority of the Chexal-Lellouche correlation over the Zolotar-Lellouche correlation can be seen in figure 5 for the TPTF experiment at high pressure (6.9 MPa) but with a low mass flux (75 kg/m²s). The void fractions calculated using the Zolotar-Lellouche correlation are overpredicted confirming the trend towards overprediction with decreasing mass flux described above. The flow regime dependent dynamic slip option is also unable to correctly predict the experimental data. This is not surprising since the Bennett [xv] map used to determine the flow regime is based on data at much higher mass flow rates. The inadequacy of this flow regime map for conditions differing from those under which it was evaluated (high pressure - high mass flow), is further displayed for the BWR4x4 experiment (figure 6). Here the mass flux is high (1400 kg/m²s) but the pressure is lower (1.0 MPa) and the flow regime dependent slip option slightly underpredicts the experimental void fraction. The predictions using the Zolotar-Lellouche and the Chexal-Lellouche correlations are almost identical and close to the experimental data, despite the lower pressure. This suggests that the overprediction observed previously only occurs for a combination of low pressure and low mass flux, with a larger dependency on the mass flow.

It should be noted that the “kinks” in the predicted void profiles shown for the BWR4x4 experiment in figure 6 are due to the relatively coarse nodalization used for this calculation.

5-EQUATION OPTION

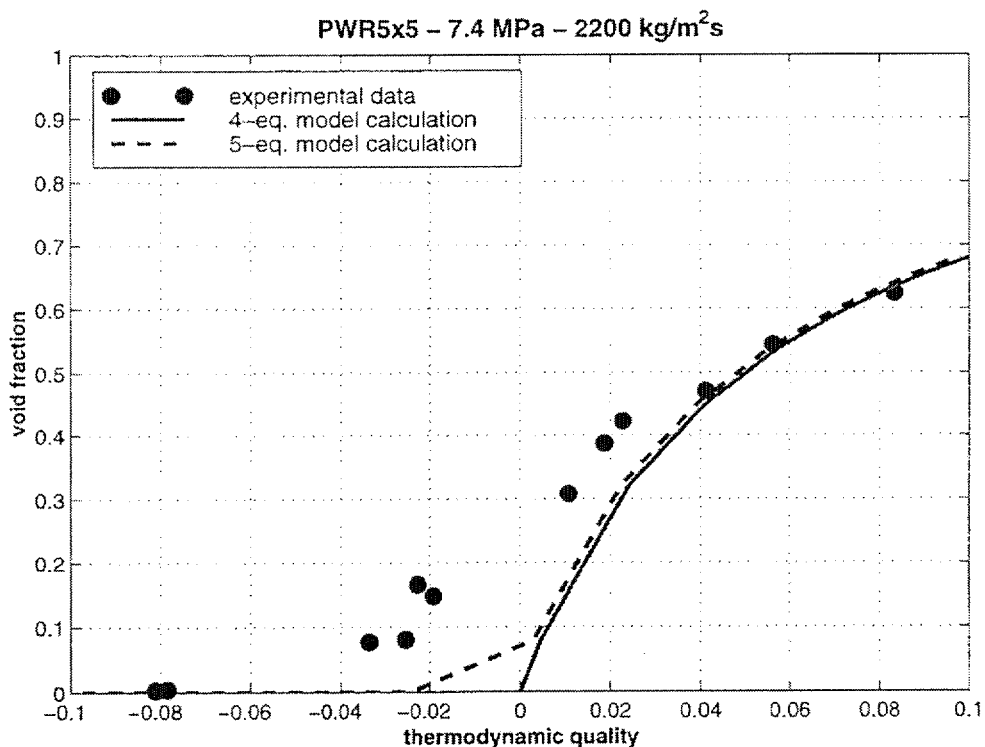


Figure 7. Prediction of a PWR5x5 experiment using the 4- and the 5-equation Chexal-Lellouche models.

As previously mentioned the slip options available when using the 5-equation model are the same as for the 3- and 4-equation models. The differences to be expected are only in areas where subcooled liquid and saturated vapor are present in the same control volume. Figure 7 compares the predictions of the 4- and 5-equation models using the Chexal-Lellouche correlation to experimental data from the PWR5x5 facility. Due to

the large amount of subcooling (see table 1) and the high mass flow rate the effect of subcooled boiling is not negligible for this experiment. The measured data shows (figure 7) that voiding begins below the elevation at which the liquid reaches the saturation temperature, i.e. the thermodynamic quality becomes positive. Both the 3-equation and the 4-equation models in RETRAN-3D force the fluid to be at saturation temperature (thermal equilibrium) in any cell where both phases are present simultaneously. Therefore it is clear that effects like subcooled boiling cannot be modeled with these options. The constraint imposed by the 3- and 4-equation models leads to the underprediction of the measured data observed in figure 7 for the 4-equation model calculation.

To overcome this limitation the 5-equation model can be used, which allows subcooled liquid and saturated vapor to be present in the same control volume. The RETRAN-3D 5-equation model was therefore used to analyze the PWR 5x5 experiments. As can be seen in figure 7 both the 4- and the 5-equation models predict the data well at qualities higher than 0.04, which is consistent with all the other comparisons at these pressure and mass flux conditions. However the subcooled void is significantly underestimated by the 5-equation model, both for negative and small positive values of the thermodynamic quality.

STEADY-STATE AND TRANSIENT SOLUTION

Figure 8 compares the predictions of the 3- and 4-equation models using the Chexal-Lellouche correlation for a NEPTUN experiment. As has been noted above, some overprediction is observed at these low pressure - low flow conditions (0.4 MPa - 42 kg/m²s). Nonetheless the predictions of both models are identical for this steady-state experiment. This is observed for all the experiments calculated using the steady-state initialization in RETRAN-3D.

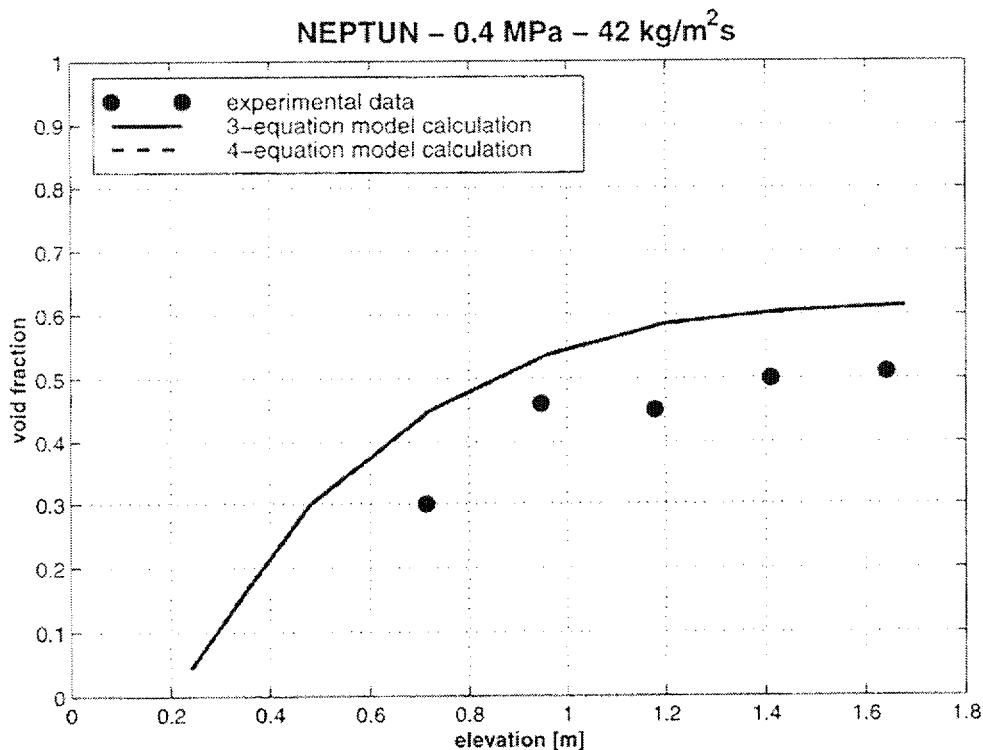


Figure 8. Prediction of a NEPTUN experiment using the 3- and 4-equation Chexal-Lellouche models.

An example of a transient experiment, THETIS boil-down, is given in Figure 9. The prediction of the collapsed liquid level is good for the initial 70 s, but after that the level falls too quickly. The reason for this rapid decrease is that the interphase drag is too high. Therefore the amount of liquid entrained in the vapor flowing out of the top of the test section is too high, leading to a more rapid decrease of liquid inventory in the test section. This effect is of the same origin as the overprediction of the void fraction by the Chexal-Lellouche correlation observed previously for steady-state experiments. The Chexal-Lellouche drift-flux model underpredicts the slip

velocity or, if the 4-equation model is used, predicts an interphase friction term which is too large, leading to the overprediction of the measured void fraction data. Since the pressure for this experiment is not particularly low (2.0 MPa), this effect is due to the very low mass flux (5 kg/m²s). Thus it is clear that not only very low pressure in combination with low mass flux, but also very low mass flux with intermediate pressure can lead to significant overprediction of the void fractions with the Chexal-Lellouche correlation.

It should be noted that similar to the predictions using the steady-state option of RETRAN-3D the differences between the 3- and the 4-equation model predictions are quite small. Therefore, it appears that when using the RETRAN-3D code to predict experiments similar to the ones analyzed here, neither of the two models is superior to the other.

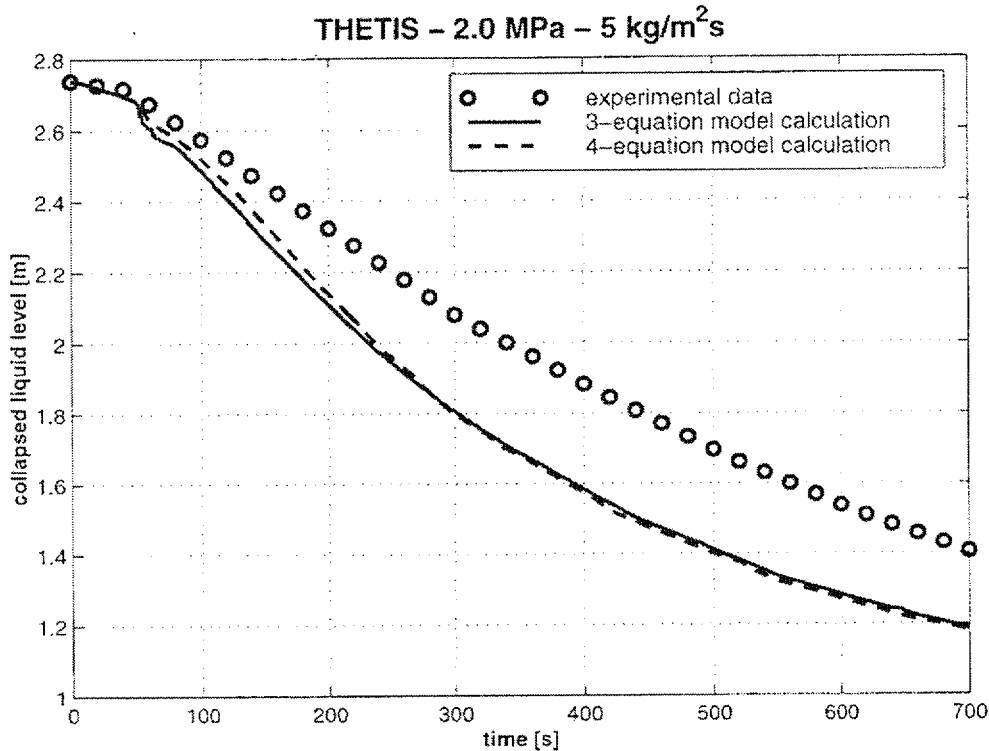


Figure 9. Prediction of a THETIS transient experiment using the 3- and 4-equation Chexal-Lellouche models.

OVERALL PREDICTION QUALITY

The consistency of the data from the different facilities, over the range of pressures from 0.5 to 7 MPa, confirms the observations made in the above sections, which are:

The comparisons presented in figures 3 to 9 show that for both the 3- and 4-equation models the option using the Chexal-Lellouche drift-flux model provides the best overall prediction. At high pressures (~ 7 MPa) and high mass flows (~1500 kg/m²s) all of the RETRAN-3D void options provide an accurate prediction. If the mass flow rate is reduced then both the Zolotar-Lellouche and the "flow regime dependent" option increasingly overpredict the data. For pressures below about 2 MPa and low mass flows (< 50 kg/m²s) the Chexal-Lellouche model also shows some overprediction. The differences between the Chexal-Lellouche correlation predictions used in the context of either the 3- or the 4-equation models and also the 5-equation model, in areas where non-equilibrium effects can be neglected, are minimal.

SPECIAL CASES

Very Low Pressure and Very Low Mass Flux

The experiments at the THETIS, PERICLES and the ACHILLES facilities with almost zero flow and at very low pressures (< 0.5 MPa) were difficult to predict using RETRAN-3D. For some experiments the steady-state initialization failed to converge for the desired inlet mass flux and pressure. The code however could be successfully initialized with a higher initial mass flow, which was then ramped down to the desired value. An example is given in Figure 10 for an experiment at the PERICLES facility. This figure shows that the transition from two-phase to single-phase vapor flow is not predicted at the same elevation for the 3- and 4-equation options. This is possibly due to the criteria in RETRAN-3D, which is set to a void fraction value of 0.999, at which a single-phase "steam" equation set is solved instead of a two-phase equation set, as well as the manner in which the cell center void fraction is extrapolated to the cell boundary. At the pressure of this experiment (0.3 MPa), this transition occurs when more than 1/3 of the mass is liquid because only 0.1 % of the volume is occupied by liquid. Clearly this is not adequate to accurately predict the correct transition elevation.

In some other cases, however, the procedure described above also failed. These were experiments with very low pressures (< 0.3 MPa) and very low mass fluxes (< 10 kg/m²s) from the ACHILLES and the THETIS facilities. The resulting solutions showed strong oscillations in the void fraction, so that no stable solution could be obtained. Reducing the rate at which the mass flux was decreased improved the results but nonetheless the void fraction oscillations were still in the order of ± 0.05 .

Similar oscillations were also observed after about 50 seconds of a null transient, of an experiment at these conditions, for which the steady-state initialization converged (Figure 11). For this experiment the initially "stable" steady-state solution becomes unstable despite leaving all the input values constant. This implies that the solution methods used in RETRAN-3D for the transient calculation are not exactly the same as those used for the steady-state initialization.

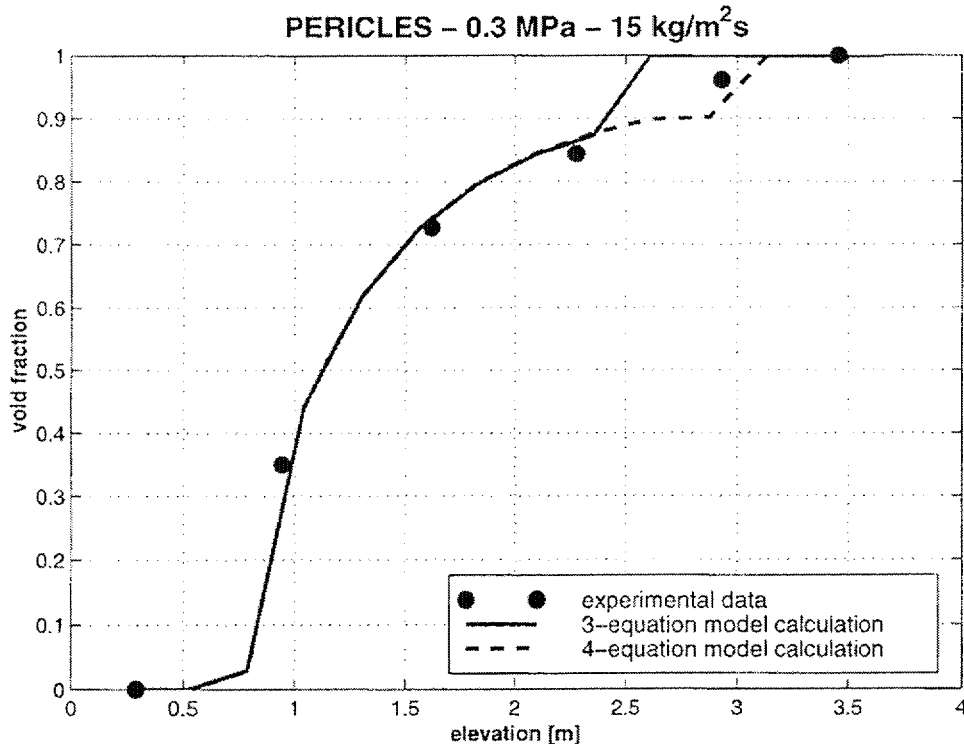


Figure 10. Prediction of a PERICLES experiment using the 3- and 4-equation Chexal-Lellouche models.

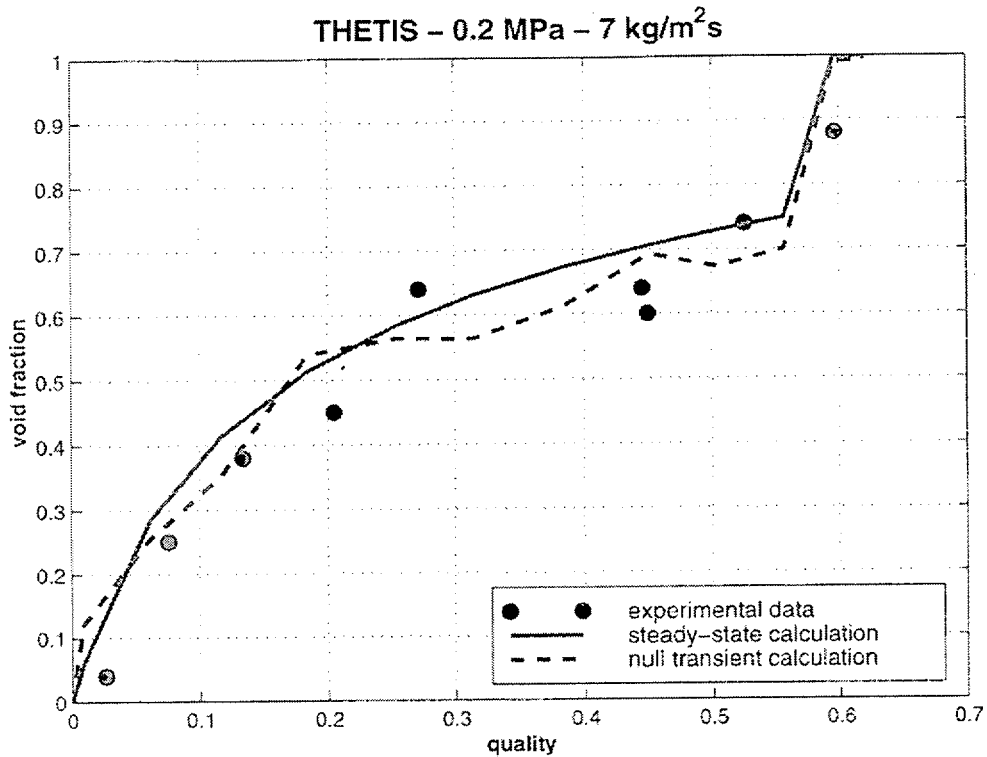


Figure 11. Prediction of a THETIS experiment using the 3-equation Chexal-Lellouche model.

VERY HIGH PRESSURE AND LOW MASS FLUX

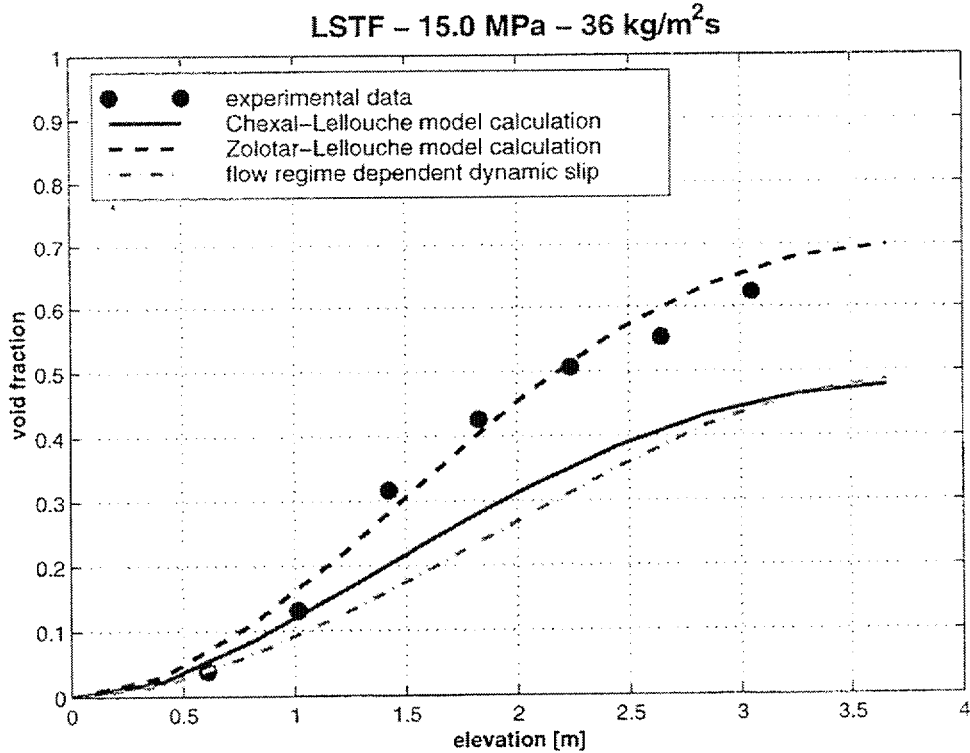


Figure 12. Prediction of a LSTF experiment using the 4-equation model options.

Figure 12 shows the RETRAN-3D predictions using the 4-equation model options for a LSTF experiment at very high pressure (15 MPa). As can be seen the Zolotar-Lellouche model is able to predict the void fractions quite accurately while the Chexal-Lellouche model and the flow regime dependent option underpredict the data. The underprediction of the measurements by the Chexal-Lellouche model is consistent with the observations reported by Anoda [vi], who evaluated the void fractions using the same correlation.

The only other data at very high pressures is from the PWR5x5 facility (up to 17 MPa), but these experiments also have much higher mass flow rates, so that a direct comparison to the LSTF experiment cannot be made. In addition the effects of subcooled boiling, which strongly effect the underprediction, are not accounted for sufficiently, as has been described above. Therefore, although it seems that data at very high pressures is underpredicted by the Chexal-Lellouche correlation, a decisive conclusion cannot be made.

GENERAL DATA PREDICTION

A comparison of all the RETRAN-3D data predictions against the measured void fractions is given in figure 13. The calculated void fractions were obtained using the RETRAN-3D 4-equation (dynamic slip) model with the Chexal-Lellouche void correlation. This figure only includes data points from experiments for which sensible predictions could be made. It therefore excludes the very low pressure (< 0.3 MPa) and very low mass flux (< 10 kg/m²s) experiments from the ACHILLES and THETIS facilities (see above). The resultant number of data points is 413, with a mean error of -0.0079 and a standard deviation of 0.0706.

In figure 13 the data from each of the experimental facilities is identified with its own unique symbol. In addition, the data at very high pressures (LSTF and PWR5x5) is separately identified (open symbols) and as previously indicated shows some underprediction. Figure 13 also shows that the results from the intermediate and low pressure experiments for low inlet flows (e.g. LSTF, NEPTUN and THETIS) show a consistent overprediction again in line with the observations made above for figures 4, 8 and 9. Therefore the trends and predictions of the selected data sets, shown in the previous figures, apply equally to all of the analyzed data.

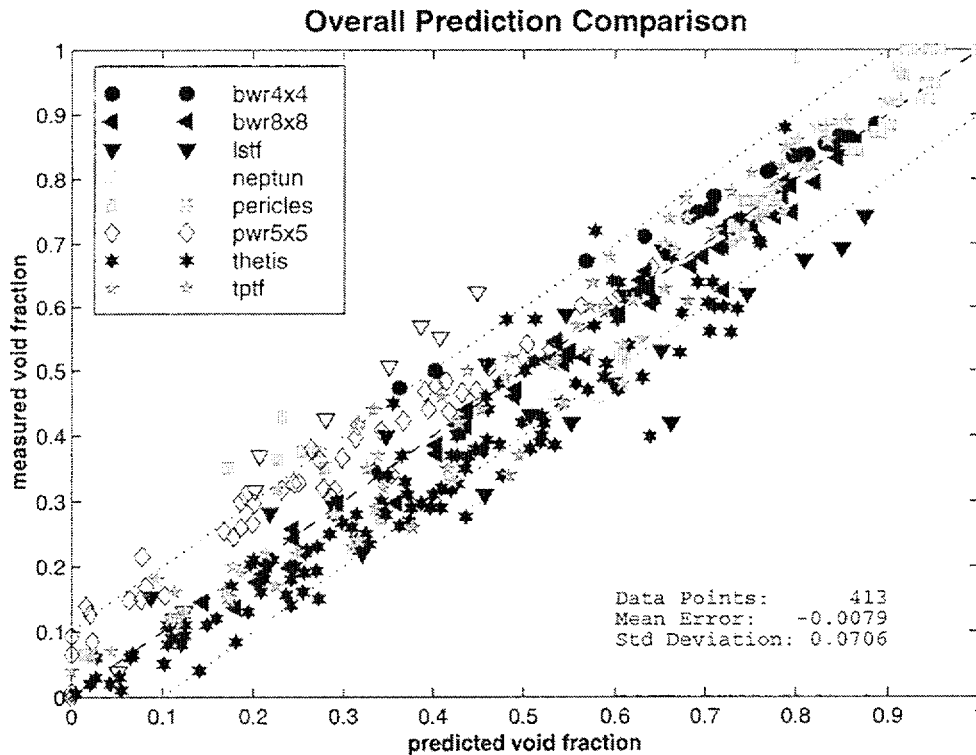


Figure 13. Overall comparison of predicted and experimental data.

CONCLUSIONS & RECOMMENDATION

Based on the simulation of a large number of rod bundle experiments from different facilities and with a wide variety of experimental parameters, several observations can be made with a high level of confidence:

- All the slip options available in RETRAN-3D can successfully and accurately predict void fractions for experiments which remain close to normal operating conditions in a BWR core. With decreasing mass flux the measured data is increasingly overpredicted by the Zolotar-Lellouche options and by the flow regime dependent dynamic slip option. The Chexal-Lellouche correlation used in either the 3- or the 4-equation model can predict data with low mass flows accurately. At very low flow ($< 50 \text{ kg/m}^2\text{s}$) and low pressure ($< 2 \text{ MPa}$) conditions, the Chexal-Lellouche drift-flux model options significantly overpredict the void. This increasing overprediction of experimental data with decreasing mass flux and to a lesser extent with decreasing pressure has been confirmed against data from several facilities at different pressures.
- In the current version of the code, RETRAN-3D cannot successfully model experiments at very low pressures ($< 0.3 \text{ MPa}$) with very low mass fluxes ($< 10 \text{ kg/m}^2\text{s}$). Under these conditions the numerical procedures either fail to converge or produce large oscillations.
- Based on the limited amount of data available at very high pressure (15 MPa) with low mass flows it appears that the Chexal-Lellouche and the "flow regime dependent" slip options significantly underpredict the experimental data. For these conditions the Zolotar-Lellouche correlation produces the most accurate results.
- Experiments for which subcooled boiling or other thermal "non-equilibrium" effects play a major role cannot be predicted with the 3-/4-equation models of RETRAN-3D. For the experiments analyzed at high pressure, high mass flows and with large amounts of subcooling, the 5-equation model with subcooled boiling, shows a significant underprediction of the void in the subcooled boiling region both for negative and small positive values of the thermodynamic quality. At higher qualities where the fluid becomes saturated the predictions of the 3-/4- and the 5-equation model are identical and show a good agreement with the experimental data.

The slip options available in the RETRAN-3D code provide a good basis for predicting the thermal-hydraulic core behavior of BWRs at normal operating conditions. For other conditions the Chexal-Lellouche drift-flux model used in the context of the 3- or 4-equation solution produces the most accurate results. For example, when compared against the total data base, the 4-equation model using the Chexal-Lellouche correlation results in a mean error of -0.008 and a standard deviation of 0.07. For transients in which very low flow conditions at low pressures play an important role, the analysis results must be carefully evaluated due to the overprediction tendency observed at these conditions by all the slip options.

ACKNOWLEDGEMENTS

This work was partly funded by the Swiss Federal Nuclear Safety Agency HSK (Hauptabteilung für die Sicherheit der Kernanlagen) and the Swiss Federal Office of Energy BFE (Bundesamt für Energie).

REFERENCES

- [i] Peterson, C. E., McFadden, J. H., Paulsen, M. P., Gose, G. C., and Shatford, J. G., 1996, "RETRAN-3D - A Program for Transient Thermal-Hydraulic Analysis of Complex Fluid-Flow Systems, Volume 1: Theory and Numerics Manual", EPRI NP-7450.
- [ii] Maier, D., and Coddington, P., 1997, "Review of Wide Range Void Correlations Against an Extensive Database of Rod Bundle Void Measurements", *Proceedings of the 5th International Conference on Nuclear Engineering*, ICONE5-2434.
- [iii] Pearson, K. G., and Denham, M. K., 1989, "Achilles Unballooned Cluster Experiments, Part 4: Low Pressure Level Swell Experiments", AEEW-R 2339.

- [iv] Mitsutake, T., Morooka, S., Suzuki, K., Tsunoyama, S., and Yoshimura, K., 1990, "Void Fraction Estimation Within Rod Bundles Based on Three-Fluid Model and Comparison with X-Ray CT Void Data", *Nuclear Engineering and Design*, Vol. 120, pp. 203-212.
- [v] Morooka, S., Inoue, A., Oishi, M., Aoki, T., Nagaoka, K., and Yoshida, H., 1991, "In-Bundle Void Measurement of BWR Fuel Assembly by X-Ray CT Scanner", *ICONE-1 Proceedings*, a-38, pp. 237-243.
- [vi] Anoda, Y., Kukita, Y., and Tasaka, K., 1990, "Void Fraction Distribution in Rod Bundle under High Pressure Conditions", *Proceedings, ASME Winter Annual Meeting, Advances in Gas-Liquid Flows*, pp. 283-289.
- [vii] Dreier, J., Analytis, G., and Chawla, R., 1988, "NEPTUN-III Reflooding and Boiloff Experiments with an LWHCR Fuel Bundle Simulator: Experimental Results and Initial Code Assessment Efforts", *Nuclear Technology*, Vol. 80, pp. 93-106.
- [viii] Deruaz, R., Clement, P., and Veteau, J. M., 1985, "Study of Two-dimensional Effects in the Core of a Light water reactor During the ECC's Phase Following a Loss of Coolant Accident", EUR 10076 EN.
- [ix] Hori, K., Akiyama, Y., Miyazaki, K., Nishioka, H., and Takeda, N., 1996, "Total Evaluation of in Bundle Void Fraction Measurement Test of PWR Fuel Assembly", *ICONE-4 Proceedings*, Vol. 1, Part B, pp. 801-811.
- [x] Jowitt, D., Cooper, C. A., and Pearson, K. G., 1984, "The THETIS 80% Blocked Cluster Experiment, Part 5: Level Swell Experiments", AEEW-R 1767.
- [xi] Kumamaru, H., Kondo, M., Murata, H., and Kukita, Y., 1994, "Void-fraction Distribution under High-pressure Boil-off Conditions in Rod Bundle Geometry", *Nuclear Engineering and Design*, Vol. 150, pp. 95-105.
- [xii] Macian, R., Cebull, P., Coddington, P., and Paulsen, M., 1998, "Implementation of an Improved Interfacial Mass and Energy Transfer Model in RETRAN-3D", *Proceedings of the Ninth International RETRAN Meeting*, Monterey, CA, June 7-10, 1998.
- [xiii] Lellouche, G. S., and Zolotar, B. A., 1982, "Mechanistic Model for Two-Phase Void Fraction for Water in Vertical Tubes, Channels and Rod Bundles", EPRI NP-2246-SR.
- [xiv] Chexal, B., Lellouche, G., Horowitz, J., Healzer, J., and Oh, S., 1991, "The Chexal-Lellouche Void Fraction Correlation for Generalized Applications", NSAC-139.
- [xv] Bennett, A. W., Hewitt, G. F., Kearsey, H. A., Keeys, R. K. F., and Lacey, P. M. C., 1965, "Flow Visualization Studies of Boiling at High Pressure", *Proc. Inst. Mech. Eng.*, Part 3C, pp. 1-11.
- [xvi] Andersen, J. G. M., and Chu, K. H., 1983, "BWR Refill-Reflood Program Constitutive Correlations for Shear and Heat Transfer for the BWR Version of TRAC", EPRI NP-1582.
- [xvii] Ishii, M., 1977, "One-Dimensional Drift Flux Model and Constitutive Equations for Relative Motion Between Phases in Various Two-Phase Flow Regimes", ANL-77-47.
- [xviii] Zuber, N., and Findlay, J. A., 1965, "Average Volumetric Concentration in Two-Phase Flow Systems", *Journal of Heat Transfer*, Vol. 87, pp. 453-468.
- [xix] Cunningham, J. P., and Yeh, H. C., 1973, "Experiments and Void Correlation for PWR Small Break LOCA Conditions", *Transactions of the American Nuclear Society*, Vol. 17, pp. 369-370.

Attachment 6

Modeling Guidelines for New RETRAN-3D Models

The numerical solution schemes used to solve the transient and steady state thermal-hydraulics problems have been revised in the RETRAN-3D computer program. The new fully implicit solution schemes replaced those from RETRAN-02; thus, any problem run with RETRAN-3D will utilize these new schemes. They apply to all of the underlying thermal-hydraulics model options including the three-, four-, and five-equation formulations with and without noncondensable gas flow. Compared with the RETRAN-02 hydrodynamic solution scheme, the implicit solution used by RETRAN-3D is more robust and faster running. Likewise, the RETRAN-3D steady-state solution generally converges faster and is also more robust than its RETRAN-02 counterpart. There is no input associated with the implicit solution algorithms.

In general, the RETRAN-3D solution scheme will run with much larger time-step sizes than RETRAN-02 because of the implicit coupling between all of the balance equations. There can be instances where the RETRAN-3D time-step size may have to be reduced to make meaningful comparisons with RETRAN-02.

A number of RETRAN-02 model improvements and new models have been added to RETRAN-3D. Many of these models are optional and for the most part do not exist in the RETRAN-02 program. Guidelines on the use of these improvements and new models are summarized below on a model-by-model basis. In some instances, models available in RETRAN-02 were improved. These models are also discussed along with the effect of the improvements.

Fanning Friction Factor for Laminar Flow

The laminar friction factor model in RETRAN-02 is computed using $16/Re$. This model is not applicable to all geometric configurations, so a general model equation is used in RETRAN-3D to define the laminar flow friction factor. The default coefficients for the general model equation give the RETRAN-02 model. Users can revise the form of the model by supplying the coefficients to the model equation. The choice must be justified on the basis of accepted models or comparison with data.

The actual transition between the turbulent and laminar friction factor models occurs where the two curves intersect in the transition region. There the turbulent friction factor is decreasing with decreasing Reynolds number and the laminar friction factor is increasing. Both friction factors are evaluated and the maximum value is used. Consequently, changing the friction factor constants from their default values will also change the transition point.

Fanning Friction for Turbulent Flow

The Fanning friction factor for turbulent flow in RETRAN-02 was computed using the Karman-Nikuradse correlation for smooth pipe. This model has been replaced with the Colebrook model in RETRAN-3D, which accounts for the effect of pipe roughness. If the wall roughness is supplied as zero, which is also the default value, the Colebrook result is equivalent to that obtained with the RETRAN-02 model.

For rough pipes, a more accurate representation of the friction factor can be obtained by supplying the wall roughness. In RETRAN-02, there was no way to account for roughness effects in the friction factor evaluation, so a modeling approach for increasing wall friction was to adjust the flow length, and thus the L/D ratio. This is not necessary in RETRAN-3D. When comparing RETRAN-02 and RETRAN-3D friction pressure drop results, care should be taken to ensure that the wall friction model inputs are consistent.

Critical Heat Flux

The default critical heat flux correlation in RETRAN-3D is the same as RETRAN-02, a pressure dependent combination of the B&W-2, Barnett, and modified-Barnett correlations. The EPRI CHF correlation is a new model in RETRAN-3D and was validated against a large body of critical flow data as reported in Reference 2. It is valid over a much wider range of pressures, flows and qualities than the individual correlations that comprise the default model. The EPRI CHF correlation is selected for use by setting IMCL=2z (or IMCR) on the 15XXXY data.

Junction Enthalpy Models

RETRAN-3D includes one new junction enthalpy model and a major revision to two others that is available in RETRAN-02. The first revised model is the enthalpy transport model.

Enthalpy Transport

The enthalpy transport model is used to account for the effects of heating on the junction enthalpy (or difference between the volume and junction enthalpies) and was originally developed to improve the accuracy of simulations using large node sizes in the heated region (3 to six in the core). It is an optional model that is activated by setting IHQCOR=1 on the Junction Data 08XXXY. With the more recent practice of using 24 nodes in BWR cores, the model becomes less important. A simple sensitivity study where the core mass inventory is compared for cases with and without enthalpy transport will give an indication of whether or not it is needed. For single phase heated regions in PWRs, the enthalpy transport model will not significantly affect the mass inventory, but it will affect the volume average temperature used for heat transfer.

In RETRAN-3D, the model has been revised to allow for multiple inlet and exit junctions, where the RETRAN-02 model only allows a single inlet and exit junction. Further, a simplifying assumption used in the RETRAN-02 solution has been eliminated in favor of a more consistent approach. RETRAN-02 makes the assumption that the mass in the half node from the volume center to the junction is half the mass in the volume. This is reasonable for a single-phase volume, but is not for a two-phase volume. In RETRAN-3D, the density distribution is directly related to the linear enthalpy distribution that the model is based on.

The more complete solution used in RETRAN-3D can lead to slightly different results, particularly when two-phase conditions exist. When making comparisons between RETRAN-02 and RETRAN-3D results, this model improvement can be the source of differences. One way to confirm that the differences are due to the improved model is to turn enthalpy transport off in both the RETRAN-02 and RETRAN-3D and then re-run the comparison analyses. If these results compare, the previous differences are related to the revised enthalpy transport model.

The model is only available for use with the three- and four-equation options. When the five-equation model is activated (see below), the enthalpy transport model is ignored, even if the enthalpy transport flag IHQCOR on the Junction Data 08XXXY is set on.

Enthalpy transport can encounter numerical difficulties when flow reversal occurs. This will typically result in a code failure. An option is available to turn enthalpy transport off at a given time or when the flow reverses. It is activated using the Enthalpy Transport Deactivation Data 080000.

Countercurrent Flow

The RETRAN-02 junction enthalpy model for countercurrent flow is based on the properties of the net flow donor volume. This can lead to aphysical subcooling and/or superheating in associated volumes. It can also lead to numerical instabilities. A model using a phasic donoring approach is used in RETRAN-3D. It is applied for the four- and five-equation models with or without noncondensable gas flow. The model eliminates the problems encountered with the RETRAN-02 model. The model is automatically activated as required by the phasic flow directions when any slip flow model is used.

Method of Characteristics

The Method of Characteristics model is a new model in RETRAN-3D that was developed to eliminate numerical diffusion from the solution of the energy equation for specific application to BWR stability analyses. The model should be applied to all heated core channels for stability analyses. It also requires the use of the five-equation model.

The model superimposes a Lagrangian solution grid on the RETRAN-3D node structure. The junction enthalpy is then obtained by interpolating between the Lagrangian mesh points that span a junction location. The Method of Characteristics Transport Data Cards 6300XX are used to activate the model. A list of junction numbers associated with the heated channel, ordered from the inlet through the exit must be supplied. Two other parameters are required, they are the minimum resolution and velocity ratio.

The resolution defines the minimum number of Lagrangian particles that will be used to describe the enthalpy (fluid property) distribution within a control volume. This minimum is applied to the volume with the highest velocity and is used to determine frequency at which new particles are created at the inlet. Volumes close to the channel inlet will have a higher density of particles because they spread out as they move toward the channel exit where the velocities are higher. A value of 5 to 7 has been found to be adequate for most applications of the model. It should be remembered that there is a trade off that must be considered when defining the minimum resolution. A large value for the resolution will define the shape of enthalpy/void fraction fronts very well but it will limit the maximum time-step size that can be taken. This is the result of the method being an explicit solution where the time-step size is limited to the Courant (or transport time) limit for the smallest node.

The velocity ratio is not used in the determination of the junction properties, other than the fact that it is used to determine the amount of auxiliary storage that is needed to store the Lagrangian grid information. If at some point during a transient solution the available storage space for the grid become inadequate, the problem will be terminated and a diagnostic message will be written indicating the cause of the failure. Should this occur, the velocity ratio can be increased to make the auxiliary storage space larger.

Choking Model

The choking model in RETRAN-3D has been modified from that used in RETRAN-02. In RETRAN-02, the donor volume pressure is used with the critical flow models to determine the flow. The junction pressure is used in RETRAN-3D, which accounts for frictional and hydrostatic losses between the volume center and the junction. This can have a significant effect for choked flow from a long volume where the friction pressure drop between the donor volume center and junction is large. The actual critical flow tables are unchanged.

By including the frictional pressure drop in the pressure used to calculate the critical flow, the pressure drop becomes a function of the critical flow. This required a revision to the numerical solution scheme. The most significant impact from a user point of view however, is the use of the junction pressure rather than the volume pressure. As a result, RETRAN-3D will typically have a lower critical flow value. The actual difference will depend on the magnitude of the frictional losses. This revision can result in differences between RETRAN-02 and RETRAN-3D computed results.

The revision to the choking model is always used in RETRAN-3D when choking is encountered. A choking model flag, JCHOKE, is set on each Junction Data Card 08XXXY as is also done in RETRAN-02. JCHOKE is used to select the choking model that will be used. A value of JCHOKE=-1 will prevent choking from being evaluated. This option is recommended for internal junctions where choking is not expected.

Control System Model

The control system model is available in both RETRAN-02 and RETRAN-3D. However, a number of functional improvements have been made in RETRAN-3D related to the control system modeling capability. First, four new blocks have been added; they are an absolute value block, a rate block, a second-order transfer function block, and a two-dimensional function generator block. The most significant improvement in the RETRAN-3D control system model is the numerical solution scheme employed to solve the governing equations for the various control blocks. In RETRAN-3D the governing equations are treated as a system of coupled equations that are solved using matrix techniques, where as RETRAN-02 uses an explicit method that simply solves one equation at a time in the order defined in the input. This may lead to a situation where the results are dependent on the block ordering.

While the improved RETRAN-3D solution method is order independent and all unknowns are updated consistently to the new time level values, it may lead to differences when attempting to perform RETRAN-02-mode (RETRAN-3D) comparisons with RETRAN-02. In the event that differences in the control system results are observed, it may be necessary to re-evaluate the RETRAN-02 control system model by using smaller time steps or rearranging the block order. Another option is to force the control system to use a smaller time-step size than the hydrodynamics.

Many control system models contain feedback loops where the output of a control block is used as the input for a previous control block. The Gauss-Seidel solution method used in RETRAN-3D may not converge for this situation. If the control system solution fails to converge, it may be necessary to

increase the iteration count, ITMAX, found on the Control System Problem Dimensions Data Card 701000.

Another approach that helps to obtain a converged solution requires a slight modification to the input model. Where feedback loops occur, the block output that is fed back should first be fed into a control input that then replaces the direct feedback signal input. This clamps the feedback input to the previous time step value, which remains constant during the Gauss-Seidel solution.

A final solution for reducing convergence problems is to reduce the convergence criterion, CNTEPS, also found on the Control System Problem Dimensions Data Card 701000. This is a quick fix that can be helpful for initial debug, but is not recommended as a long-term solution.

Four-Equation or Slip Modeling

The four-equation or slip model is used to account for differences between the phasic velocities for two-phase conditions. RETRAN-02 contained two slip models, the dynamic slip model based on the difference between the phasic momentum equations and the algebraic slip model based on the Zolotar-Lellouche drift flux model. These modeling capabilities are retained in RETRAN-3D, but they have been augmented by a number of improvements.

The method used to obtain the junction properties for countercurrent flow has been enhanced for all slip models. It is discussed with the junction enthalpy models.

In the RETRAN-3D dynamic slip model, the form losses have been included in the dynamic slip equation. They were neglected in RETRAN-02. This improvement can lead to differences between RETRAN-02 and RETRAN-3D results, although the effect is generally negligible. The most significant change related to the dynamic slip equation is the numerical solution method. Where RETRAN-02 used an explicit scheme that introduced significant time-step size restrictions, RETRAN-3D employs an implicit scheme that remains stable for large time-step sizes. This is the primary area of impact for RETRAN-3D users.

The Zolotar-Lellouche model used in RETRAN-02 was valid only for cocurrent upflow conditions typical of BWR cores. A more accurate model, covering a wider range of geometries and flow conditions was implemented in RETRAN-3D as an option. It is referred to as the Chexal-Lellouche model and produces results that are very close to those of the Zolotar-Lellouche model for BWR applications. The Chexal-Lellouche model is based on a larger database that has been used to extend the range of application to other geometries and flow patterns. It is the recommended default slip model for RETRAN-3D. It is selected by setting ISFLAG=3 on the Problem Dimension Data 01000Y.

The dynamic slip model uses flow field models and a flow regime map to model interphase friction. An option has been added to allow a drift flux correlation to be used to determine interphase friction. It is similar to the models used by RELAP5 and TRAC. Either the Zolotar-Lellouche or the Chexal-Lellouche models can be used by setting ISFLAG=4 or ISFLAG=5 on the Problem Dimension Data 01000Y, respectively. This model will reproduce the corresponding algebraic slip model results for steady-state conditions. It will however include the temporal effects of the added mass term and pressure gradient ignored by the algebraic model. For this reason, this model could be a better choice for more severe transient analyses. Currently, the model should not be used for horizontal regions.

Dynamic Flow Regime

The dynamic flow regime model is used in conjunction with the dynamic slip model. It uses an additional differential equation to determine the interfacial area required for the interphase momentum and energy exchange. It was included in RETRAN-3D as a developmental model that can be used for further research activities and is an optional model that is activated by setting ISFLAG=6 on the Problem Dimension Data 01000Y. The dynamic flow regime model is not intended for use in licensing related analyses.

Five-Equation Model

The five-equation model accounts for the effects of thermodynamic nonequilibrium and should be used when conditions will exist where cold fluid will be injected into a two-phase volume or when subcooled boiling is expected. It is activated by setting NEWEQS=1 and IHTMAP=1 on the Problem Dimension Data 01000Y. A slip model (ISFLAG=1, 2, 3, 4, or 5 on the Problem Dimension Data 01000Y) must be specified as well.

In RETRAN-02, the void profile fit model was developed to predict the effect of subcooled boiling on density reactivity feedback. It is used with the four-equation model and does not directly affect the thermal-hydraulic conditions other than how the density reactivity affects the core power. In contrast, the void profile fit model is not used when the five-equation model is active (IVOID=1 on the Problem Dimension Data 01000Y). The five-equation model directly accounts for subcooled boiling effects that are included in the thermal-hydraulics and reactor kinetics.

An implicit assumption used to close the five-equation model is that when two-phase conditions exist, the liquid can be subcooled, saturated, or superheated, but the vapor is saturated. When vapor only conditions exist, the vapor can be saturated or superheated. If liquid is injected into a superheated vapor volume, the water will be mixed instantaneously, de-superheating the vapor. Liquid will appear only when the vapor reaches the saturation point.

When the five-equation model is used, the wall and interphase mass transfer models are chosen automatically, based on the local flow conditions. The Lellouche model is used to compute subcooled boiling and the related mass transfer. It effectively partitions the wall heat transfer between the liquid heating and boiling components, giving the mass transfer rate. Likewise, when condensation occurs, the associated heat transfer is used to define the mass transfer rate. The interphase mass transfer processes are based on flow regime models and regime dependent correlations for the interfacial area and heat transfer coefficient. These correlations have been validated for subcooled boiling, ECC injection, rapid depressurization (flashing) and BWR pressure increase transient scenarios. The validation work confirms that the models reasonably predict the behavior for these types of transients.

Noncondensable Gas Flow

The noncondensable gas flow option was added to RETRAN-3D to allow situations to be modeled where noncondensable gas is present and flows through the system. When the option is used, noncondensable gas can be present at steady state, or it can appear as the result of the accumulator

component draining or via a junction flow boundary condition where the junction fluid is defined to be a noncondensable gas.

When the noncondensable flow option is used, the appropriate thermodynamic state and transport properties are computed automatically for conditions ranging from pure noncondensable gas to mixtures of water and noncondensable gas. The option is compatible with the three-, four-, and five-equation models. For all of these models, the humidity is assumed to be 100%. The pressurizer model currently does not account for noncondensable gas that may flow into it.

The wall heat transfer models in RETRAN-3D have been revised to account for the presence of noncondensable gas. By default, the Dittus-Boelter correlation will be used to model convective heat transfer to noncondensable gas. An option is available on the Heat Conductor Data 15XXX_Y that causes the Catton-Swanson correlation to be used for convective heat transfer to noncondensable gas. The effect of noncondensable gas on boiling heat transfer is neglected. If condensation heat transfer is encountered in a volume that also contains a noncondensable gas, the Siddique and Chun-Seban correlations are automatically selected to account for the presence of noncondensable gas.

A number of separate effects tests have been analyzed using the noncondensable gas flow option. Based on the results of these analyses, the models appear to be modeling the presence of noncondensables accurately. However, no validation analyses have been made of a large system, although a mid-loop example problem indicates that the models are functioning in a reasonable and intuitive manner.

Fluid Dynamics Equations Iterative Solution Scheme

RETRAN-3D has two methods for solving the matrix equations associated with the solution of the thermal-hydraulics balance equations. The first is a direct solution that uses a block elimination technique. The other is an iterative solver that can be used to improve running time for large problems.

The iterative solution scheme for the fluid dynamics equations was developed for problems that involve a multiple-channel thermal-hydraulic core model, generally used in conjunction with the 3D-kinetics model. This iterative scheme is especially efficient compared with the block elimination solution method when there are a large number of core channels or when the steady-state flow calculation option is used. It is recommended that the user choose the iterative solution scheme if the core model consists of more than 20 hydraulic channels, or the steady-state flow calculation (flow splits) is used for initialization. It is activated by setting NSOL34=2 on the Problem Dimension Data 01000_Y.

Steady-State Initialization

The default steady-state initialization feature in RETRAN-3D is similar to the one in RETRAN-02 and they have similar input requirements for specifying the initial conditions. The major difference between the two lies in the numerical solution method. RETRAN-02 is an explicit scheme and RETRAN-3D is implicit. Where RETRAN-02 solves the junction flow and slip equations one at a time and the energy equations in a coupled matrix, RETRAN-3D solves all of the balance equations in a single matrix. For single-phase problems, this coupling doesn't significantly improve convergence because the coupling between the flow and energy equations is weak. However, when two-phase conditions exist, the implicit RETRAN-3D solution converges faster and has fewer situations where it

doesn't converge. The steady-state initialization feature includes all of the underlying balance equations that the user selects, e.g. the base three-equation formulation plus slip, vapor continuity, and/or nocondensable gas continuity. The input option to request use of the steady-state feature and the governing equation selection is on the Problem Dimension Data 01000Y.

Several new steady-state initialization features are optionally available in RETRAN-3D. They are the low power steam generator initialization option and the steady-state flow split option. Each is discussed below.

Low Power Steam Generator Initialization

The standard steady-state initialization option, also referred to as the RETRAN-02 method, will adjust the steam generator conductor areas to achieve the correct total energy transfer rate. In some instances, particularly for low power initialization, the amount of the heat transfer surface area adjustment may be unacceptable. In addition, the heat conduction solution is not solved simultaneously with the energy, momentum and dynamic slip equations, which can cause steady-state convergence problems in the steam generator. In the low power steady-state solution scheme, the steady-state heat conduction and fluid equations are solved together in finite difference form. With this option the steam generator heat conductor area will not be adjusted. However, either the secondary-side pressure or inlet enthalpy to the tube bundle on the secondary side will be adjusted (based on user selection) to achieve an overall primary to secondary energy balance. The model is optionally selected by use of the Low Power Steam Generator Steady-State Initialization Input Cards 2350XY.

There are some practical limitations as to how much influence either the pressure adjustment or the inlet enthalpy adjustment will have on the overall energy balance and the user must supply reasonable estimates for initial conditions and must have reasonable expectations of this scheme. As an example, if the shell side of the tubes is mostly two phase, a secondary-side pressure adjustment will have the most direct influence on the heat transfer rate since the pressure determines the secondary temperature. An enthalpy adjustment would have some effect but it would be much less than pressure adjustment. Consequently, pressure would be the logical choice for the code to adjust. There is a practical limit to how much the pressure can be adjusted to change the heat transfer rate. If the pressure were increased to the point that all the fluid is subcooled, further adjustment would be meaningless. If this occurs, the user must review the consistency of the input.

If the shell side is mostly subcooled liquid or superheated vapor, the logical choice for the user is to allow the code to adjust bundle inlet enthalpy since it would have a direct effect on secondary temperature. In this situation, pressure adjustment would have only a minor influence on the energy transfer rate. Consequently, it is incumbent on the user to select the appropriate parameter for adjustment and to review the amount of adjustment to be sure it is reasonable.

The user has the option to provide an initial estimate of the fraction of the total power that is removed from the primary system by each conductor, or to use an initial estimate based only on the ratio of the conductor heat transfer area to the total steam generator heat transfer area. The area ratio approach is generally adequate for full power conditions in U-tube and once-through steam generators and in some low power U-tube cases. An initial estimate based on the expected energy removal fractions is generally required for low power once-through cases. When the user supplies the initial estimate of the energy removal profile, the data are supplied on a conductor-by-conductor basis, beginning with the conductor at the inlet entrance of the secondary side. In a once-through steam generator, this is the

conductor at the bottom of the conductor stack. In a U-tube steam generator, the first conductor is the same as the one associated with the first conductor in the tube region on the primary side.

With this option, the user specifies the type of steam generator being modeled, whether the secondary pressure or bundle inlet enthalpy is to be adjusted, the volume number in which the secondary pressure is supplied and an optional initial estimate for energy transfer distribution through the steam generator conductors.

Flow Split Option

The base or RETRAN-02 steady-state initialization scheme requires the junction mass flow rates to be supplied as initial conditions. This implies that the flows are always known. For some situations the flows aren't known, for example a detailed core model with many parallel channels. A new feature is available in RETRAN-3D that will allow the steady-state flows to be computed for parallel flow paths. Where the RETRAN-02 steady-state method requires a loss coefficient to be computed for all (or all but one) of the parallel channels, the flow split option uses the loss coefficients and pressure drop across the channels to determine the individual channel flows.

Currently, the parallel channels must be closed, i.e. no cross flow connections are allowed, and the channels must be connected to common inlet and exit volumes, e.g. the lower and upper plenum volumes. The option is requested using the JESTW=2 flag on the Junction Initial Condition Specification Data Card 232XXX. When using the flow split option, an estimate for the channel flow is required for use as a starting point. Initial flow estimates must be specified such that the mass balance is satisfied, otherwise the problem will be terminated.

Accumulator Model

The RETRAN-3D accumulator model is a component model, new to RETRAN-3D that is designed to simulate the response of a PWR accumulator. It accounts for the fact that the expanding noncondensable cover gas (generally nitrogen) will cool below the temperature of the liquid region. The cover gas expansion is modeled as a polytropic expansion of the noncondensable cover gas. RETRAN-02 does not have the capability to model an accumulator with a noncondensable gas above a liquid region, where thermal nonequilibrium develops between them as the accumulator drains.

Use of the accumulator model in RETRAN-3D is optional and is used by setting NACC on the Problem Dimension Data 01000Y. The necessary Accumulator Data Cards 620XXX must also be supplied.

The geometry of the accumulator volume can influence the selection of a user-defined constant used by the model. Reference 1 indicated that the surface to volume ratio of the accumulator vessel could affect the value of the polytropic expansion coefficient that should be used. The following summarizes the expansion coefficient obtained for data comparisons for three different experiments with different surface to volume ratios.

<u>System</u>	<u>A_{surf}/V (m^{-1})</u>	<u>Expansion Coefficient</u>
Semiscale	16.6	1.11
LOFT	5.8	1.31

The noncondensable gas mixture defined for the system, whether allowed to default or defined through user input, is used as the accumulator cover gas. At steady state, the liquid cover gas are assumed to be at a common temperature and pressure, which are input on the Volume 05XXXY or the Initial Volume Thermodynamic Condition Data 231XXX, respectively. The initial level of the liquid-gas interface is relative to the bottom of the accumulator volume.

The accumulator model can be used regardless of the use of the noncondensable flow option that allows noncondensable gases to move through a hydrodynamic system. If the noncondensable flow option is not used, the code will fail or produce incorrect results when the accumulator drains. In this mode of operation, it is common practice to close the accumulator valve before it drains. When the noncondensable gas flow option is active, noncondensable gas will flow from the accumulator once all liquid is removed.

If an air region is modeled in a RETRAN-02 separated volume above a liquid region, it is not equivalent to the RETRAN-3D accumulator model. The RETRAN-02 equation of state for air-water mixtures assumes that the cover gas and liquid are at the same temperature. This artificially removes energy from the liquid to heat the air to the liquid temperature. As a result of this isothermal assumption, the accumulator pressure will be in error on the high side, leading to injection flow rates that are also high.

Dynamic Gap Conductance Model

The dynamic gap conductance model optionally available in RETRAN-3D, accounts for the effects of fuel and cladding deformation on the gap conductance. Three modes of heat transport are permitted in the model, i.e., radiation, conduction in the fill gas, and contact conduction when the pellet is in physical contact with the cladding. Use of the model is requested by setting NGAP on the Problem Dimension Data 01000Y. The necessary Dynamic Gap Conductance Data Cards 225XXY must also be supplied.

The model accounts for the effects of thermal expansion of both fuel pellet and cladding on gap dimensions and fill gas pressure and the effect of pressure (internal and external) on the gap dimensions. The fill gas mixture may contain up to six components. Phenomena other than temperature affecting the rod geometry such as pellet fracturing have been neglected. Although the heat conduction model and portions of the gap conductance model are both derived for one dimensional geometry, use of the dynamic gap conductance model in RETRAN-3D requires use of a conductor stack since all of the conductors in a stack are included in the gas pressure calculation. Otherwise, the calculations are one-dimensional (radial).

The fill gas composition must be supplied as input data on the Dynamic Gap Conductance Model Data Cards 225XXY. It should be obtained from a fuel performance code that computes the change in the fill gas composition as a function of the fuel power history. The cold pin pressure is also required as are the fuel pellet and cladding surface roughnesses, the plenum and gap geometric descriptions.

The dynamic gap model should be used when a best estimate calculation of the gap conductance value is wanted. However, the input requirements are much more demanding and require input from a steady state fuel performance code.

Attention should be directed to comparisons between the initial temperatures predicted by RETRAN-3D and those predicted by the fuel performance code to ensure that they are in agreement, indicating a consistent problem specification.

Multidimensional Kinetics

The choice to use the multi-dimensional kinetics (3D kinetics) model involves identification of the source for the cross section model and associated data and methods for coupling the kinetics model to the thermal hydraulics model in the reactor core.

The decision to use the 3D-kinetics model should be based on the consideration of resources and the real need for the model. If the reactor core is symmetric and the transient forcing functions are core-wide then a lower order kinetics model might be sufficient. Examples of cases in which a 3D kinetics model should be considered are; motion or location of high worth control rods in a non-central location, core flow or other core boundary condition disturbances in a non-uniform manner, or a tightly coupled kinetic-thermal hydraulic feedback event that is not core-wide. Typical transients that represent these, respectively, are; rod eject or rod withdrawal from a non-central location, PWR main steam-break and BWR regional stability transients.

There are many other situations that may require the 3D kinetics model and the user must weigh the cost of generating the data and the subsequent analysis effort against the desired result. Generally, if detailed, localized information is needed, or if it is not clear how to apply conservative assumptions to a lower order kinetics (i.e. point or one-dimension) model, then the decision for a 3D kinetics model should be considered.

Cross Section Model and CDI file

The cross section model in RETRAN-3D is based on the format used in the CORETRAN [3] code. The cross-section file for RETRAN-3D includes the core dimensions, core fuel loading information, and a three-dimensional nodal cross-section database. The database format is basically a 'Tables' type of model where the cross section dependencies are given as functions of instantaneous thermal-hydraulics parameters such as moderator density and fuel temperature, and mechanical effects such as control rod motion or soluble boron insertion.

An additional data file that contains the core geometric description (the CDI file) is used by the channel model described below. The file is generated by CORETRAN and is in ASCII format.

If CORETRAN is not available, then the user must provide a data translator to convert the cross section data into the RETRAN-3D format. The fuel loading and depletion data must be obtained from a multidimensional core simulation code such as CORETRAN or SIMULATE-3[4] and the nodal cross-section database must be generated from advanced lattice codes such as CPM-3[5] or CASMO-4.[6] A way to provide the CDI file must also be developed.

The cross-section file used by the multidimensional kinetics option is binary. A description of the cross section file and the CDI file and its contents can be found in the RETRAN-3D Programmer's Manual.

Spatial Detail

RETRAN-3D uses the concept of a channel model to couple the kinetics and thermal hydraulics in the core. A channel in this context is a stack of connected control volumes, junctions, and conductors that comprise an axial flow path through the core.

A collection of channels can form a complex, interconnected flow field in a RETRAN-3D core, but the simplest element is a channel. Through the use of this model, the user is no longer required to supply the individual volume, junction, and conductor data within the channel. The user will specify a small amount of data to characterize the channel and options used in all of the elements of the channel, and RETRAN-3D will expand and unfold this data internally into the conventional volume and junction connection matrix.

The channel model is used in the following way. The user supplies all of the problem dimension information on the Problem Dimension Data Card 01000Y for the system model, excluding the active core. The channel model will compute the required nodal values and correct the dimensional data. A channel model is used to describe that portion of the kinetics model that forms the feedback basis for the neutronics calculation. The channel conductor temperatures are used to form the fuel temperature dependent cross sections and the channel fluid density or void fraction is used to form the moderator feedback.

The user has complete freedom about how to 'overlay' the thermal-hydraulic channels onto the neutronic nodes. The core is usually represented neutronically as individual fuel assemblies while a channel can be used as a 'one-to-one' or more course (i.e., one channel for many neutronics) representation.

Previous nodalization studies indicate that the RETRAN-3D execution time is nearly a linear function of the total number of control volumes and junctions. Since a typical core region may consist of several hundred volumes and junctions, there may be a practical upper limit to the number of channels that can be used in the core region. Ideally, there is a single RETRAN-3D control volume for each neutronics node. This means that there is a one-for-one correspondence between the thermal-hydraulics nodalization and the neutronics spatial overlay. In practice, this may not be the case and a RETRAN-3D core channel may represent more than one neutronics fuel assembly. In fact a RETRAN-3D channel can represent from one to many (ten to hundreds) assemblies.

In this situation, a RETRAN-3D channel will supply the same feedback information to all of the neutronics assemblies contained within. On the other hand, the power fractions calculated by the detailed kinetics are averaged, over the volume, to provide an averaged power fraction to the corresponding RETRAN-3D channel.

In the construction of the overlay the analyst is typically guided by information about what part of the core is changing most rapidly, adding channels where most of the nonsymmetrical behavior is expected or where parameters of interest are required. In some cases, previous analyses with detailed steady-

state physics codes or transient core codes yield information about the construction of the thermal-hydraulics layout.

Numerical Options

The RETRAN-3D neutronics model is based upon the analytic nodal method as outlined in Section 3.0 of Chapter V of the RETRAN-3D theory manual. The method formed the basis of the solution methods for the ARROTTA and CORETRAN codes and the numerical analysis methods contained in those programs and adapted for use in RETRAN-3D.

An alternative solution method to the 'original' CORETRAN ANM technique has been developed by Downar, et. al., at Purdue[7] that can result in significant reduction in computational times. This is referred to as the PARCS method and was developed by merging state-of-the-art methods such as the nonlinear nodal method with numerous improvements over the existing methods resulting in a unique, highly efficient set of spatial kinetics solution methods.

The user has a choice of these two solution schemes to select. Experience has shown that the PARCS method is considerably faster than the default ANM method in many cases but the user should examine the two methods on a case by case basis to demonstrate consistency in results.

Limitations

One of the assumptions in the nodal method is that the group fluxes are continuous across nodal interfaces and, thus, the face averaged nodal fluxes must also be continuous. However, a number of approximations (homogenized nodal compositions, diffusion theory relationship between currents and flux gradients, and shapes of the transverse leakages) are made in developing the relationships for a given node among the volume averaged fluxes, face averaged fluxes, face averaged currents, and average transverse leakages that may lead to violations of the continuity assumption. Discontinuity factors at nodal faces are introduced to reduce the discontinuities in the face averaged flux values across the nodal interface. These discontinuity factors are computed a priori to using the ANM option in the RETRAN-3D program. A limitation in the model is that the factors are independent of the nodal void content.

References

1. V. T. Berta and D. L. Reeder, "ECCS accumulator Performance in Scaled PWR Experiments", Proceedings: ANS Winter Meeting – Washington, D. C., November 1978.
2. Reddy, P. G., and Fighetti, C. F., "Parametric Study of CHF Data, Volume 2; A Generalized Subchannel CHF Correlation for PWR and BWR Fuel Assemblies", EPRI NP-2609, 1983.
3. Dias, A. F., et al., "CORETRAN-01 - A Three-Dimensional Program for Reactor Core Physics and Thermal-Hydraulics Analysis", User's Manual, EPRI WO-3574, October 1997.
4. "SIMULATE-3 - Advanced Three-Dimensional Two-Group Reactor Analysis Code", User's Manual, Studsvik/SOA-95/15, Revision 0, October 1995.

5. Jones, D. B., et al, "CPM-3 - A Core Physics Module for the Analysis of Nuclear Fuel Assemblies Using Arbitrary Geometry Modeling", User's Manual, EPRI RP-3418, October 1997.
6. Edenius, M., et al., "CASMO-4 - A Fuel Assembly Burnup Program", User's Manual, Studsvik/SOA-95/1, Revision 0, September 1995.
7. Joo, H. G., Jiang, G., Barber, D. A., Downar, T. J., "PARCS - A Multi-dimensional Two Group Reactor Kinetics Code Based on the Nonlinear Analytic Nodal Method", PU/NE-91-4, 1977.